Physics Letters B 724 (2013) 213–240

Contents lists available at SciVerse ScienceDirect

Physics Letters B

www.elsevier.com/locate/physletb

Multiplicity and transverse momentum dependence of two- and four-particle correlations in pPb and PbPb collisions

CMS Collaboration *

CERN, Switzerland

ARTICLE INFO

Article history:
Received 3 May 2013
Accepted 15 June 2013
Available online 24 June 2013
Editor: M. Doser

Keywords:
CMS
Physics
Heavy ions

ABSTRACT

Measurements of two- and four-particle angular correlations for charged particles emitted in pPb collisions are presented over a wide range in pseudorapidity and full azimuth. The data, corresponding to an integrated luminosity of approximately 31 nb^{-1}, were collected during the 2013 LHC pPb run at a nucleon–nucleon center-of-mass energy of 5.02 TeV by the CMS experiment. The results are compared to 2.76 TeV semi-peripheral PbPb collision data, collected during the 2011 PbPb run, covering a similar range of particle multiplicities. The observed correlations are characterized by the near-side ($|\Delta\phi| \approx 0$) associated pair yields and the azimuthal anisotropy Fourier harmonics (v_n). The second-order (v_2) and third-order (v_3) anisotropy harmonics are extracted using the two-particle azimuthal correlation technique. A four-particle correlation method is also applied to obtain the value of v_2 and further explore the multi-particle nature of the correlations. Both associated pair yields and anisotropy harmonics are studied as a function of particle multiplicity and transverse momentum. The associated pair yields, the four-particle v_2, and the v_3 become apparent at about the same multiplicity. A remarkable similarity in the v_3 signal as a function of multiplicity is observed between the pPb and PbPb systems. Predictions based on the color glass condensate and hydrodynamic models are compared to the experimental results.

1. Introduction

Studies of multi-particle correlations play a major role in characterizing the underlying mechanism of particle production in high-energy collisions of protons and nuclei. Of particular interest in relativistic nucleus–nucleus (AA) collisions is the observed long-range (large $|\Delta\eta|$) structure in two-dimensional (2D) $\Delta\eta$–$\Delta\phi$ correlation functions. Here, $\Delta\phi$ and $\Delta\eta$ are the differences in azimuthal angle ϕ and pseudorapidity $\eta = -\ln[\tan(\theta/2)]$ between the two particles, where the polar angle θ is defined relative to the beam axis. One source of such long-range correlations is the "elliptic flow" induced by the hydrodynamic evolution of the lenticular collision zone in non-central nucleus–nucleus interactions [1]. Elliptic flow contributes a $\cos(2\Delta\phi)$ component to the two-particle correlation function over a broad $|\Delta\eta|$ range [2]. The studies of elliptic flow have been carried out over a wide range of energies and collision systems [3–11].

After subtracting the elliptic flow component, a pronounced correlation structure at $|\Delta\phi| \approx 0$ (near-side) extending over large $|\Delta\eta|$ remains in AuAu collisions at the Relativistic Heavy Ion Collider (RHIC) [12–15]. Such long-range near-side correlations are not reproduced by models of nucleon–nucleon interactions such as PYTHIA, and are not observed in pp collisions at RHIC energies. A variety of theoretical models were proposed to interpret this residual long-range near-side correlation as a consequence of jet-medium interactions [16–21]. However, it was later realized that, because of event-by-event fluctuations in the initial-state collision geometry [22–24], higher-order anisotropic flow components could also be induced, in particular the "triangular flow" which contributes a $\cos(3\Delta\phi)$ component [25–30]. Therefore, the observed long-range $\Delta\eta$ correlations in AA collisions can, in general, be attributed to the collective expansion of a strongly-interacting medium. The detailed azimuthal correlation function is typically characterized by its Fourier components, $\sim 1 + 2\sum_n v_n^2 \cos(n\Delta\phi)$, where v_n denote the single-particle anisotropy harmonics [31]. In particular, the second (elliptic) and third (triangular) Fourier harmonics are assumed to most directly reflect the medium response to the initial collision geometry and to its fluctuations, respectively. Detailed studies of elliptic and triangular flow provide insight into fundamental transport properties of the medium [26,27,32]. The long-range correlations and anisotropy Fourier harmonics have also been extensively studied in PbPb collisions at the Large Hadron Collider (LHC) [9–11,33–37].

Recently, a similar long-range near-side correlation structure (without subtraction of any flow component) was observed in the highest particle multiplicity proton–proton (pp) [38] and

* *E-mail address:* cms-publication-committee-chair@cern.ch.

0370-2693/
http://dx.doi.org/10.1016/j.physletb.2013.06.028

proton–lead (pPb) [39] collisions at the LHC. In pPb collisions, the overall strength of the near-side correlation is found to be significantly greater than in pp collisions. The away-side ($|\Delta\phi| \approx \pi$) correlations contain substantial contributions from the back-to-back jets, and thus have not been the focus of these initial studies. A procedure for removing the jet correlations on the away side by subtracting the correlations for very-low-multiplicity data was recently introduced [40,41], and used to study the long-range correlations in pPb on both near and away sides using the anisotropy Fourier harmonics. Evidence of such correlations was also found recently in 200 GeV deuteron–gold collisions at RHIC [42]. While hydrodynamic flow is the commonly accepted explanation of such long-range correlations in the AA collision systems, a variety of theoretical models have been proposed to explain the origin of this phenomenon in small collision systems like pp (see Ref. [43] for a recent review) and pPb. Such models include gluon saturation in the initial interaction of the protons and nuclei [44,45] and hydrodynamic effects in the high-density systems possibly formed in these collisions at TeV energies [46,47]. Since hydrodynamic flow is intrinsically a multi-particle phenomenon, it can be probed more directly using multi-particle correlation (or cumulant) techniques [48] rather than with two-particle correlations. In particular, two-particle correlations, arising from jet production, are expected to be strongly suppressed using the multi-particle method. A measurement of an elliptic flow signal using the four-particle cumulant method in pPb collisions was recently presented [49].

To provide further constraints on the theoretical understanding of the particle production mechanisms in different collision systems, this Letter presents a detailed analysis of two- and four-particle angular correlations in pPb collisions at $\sqrt{s_{NN}} = 5.02$ TeV. This 2013 data set, especially with the implementation of a dedicated high-multiplicity trigger, provides a much larger sample of very-high-multiplicity pPb events. Therefore, correlations can be explored up to a multiplicity comparable to that in mid-central PbPb collisions (e.g., ∼55% centrality, where centrality is defined as the fraction of the total inelastic cross section, with 0% denoting the most central collisions). The two-particle long-range correlation data are presented in two different but closely-related approaches: the near-side associated yields, which characterize the absolute yield of correlated particle pairs, and anisotropy harmonics (v_2 and v_3), which provide a measurement of relative correlation magnitude with respect to the uncorrelated background. To further investigate the multi-particle nature of the correlations, a four-particle cumulant analysis is also performed for determining the v_2 harmonic. Both the associated yields and anisotropy harmonics are studied as a function of particle multiplicity and transverse momentum, providing a direct comparison of pPb and PbPb collision systems over a broad range of similar multiplicities.

2. Experimental setup

The CMS detector comprises a number of subsystems and a detailed description can be found in Ref. [50]. The results in this Letter are mainly based on the silicon tracker information. This detector, located in the 3.8 T field of the superconducting solenoid, consists of 1440 silicon pixel and 15 148 silicon strip detector modules. The silicon tracker measures charged particles within the pseudorapidity range $|\eta| < 2.5$, and provides an impact parameter resolution of ≈15 μm and a transverse momentum (p_T) resolution better than 1.5% up to $p_T \approx 100$ GeV/c. The electromagnetic calorimeter (ECAL) and hadron calorimeter (HCAL) are also located inside the solenoid. The ECAL consists of 75 848 lead-tungstate crystals, arranged in a quasi-projective geometry and distributed in a barrel region ($|\eta| < 1.48$) and two endcaps that extend to $|\eta| = 3.0$. The HCAL barrel and endcaps are sampling calorimeters composed of brass and scintillator plates, covering $|\eta| < 3.0$. Iron/quartz-fiber Čerenkov hadron forward (HF) calorimeters cover the range $2.9 < |\eta| < 5.2$ on either side of the interaction region. The detailed Monte Carlo (MC) simulation of the CMS detector response is based on GEANT4 [51].

3. Selections of events and tracks

This analysis is performed using data recorded by CMS during the LHC pPb run in 2013. The data set corresponds to an integrated luminosity of about 31 nb^{-1}, assuming a pPb interaction cross section of 2.1 barns. The beam energies were 4 TeV for protons and 1.58 TeV per nucleon for lead nuclei, resulting in a center-of-mass energy per nucleon pair of 5.02 TeV. The direction of the higher energy proton beam was initially set up to be clockwise, and was then reversed. As a result of the energy difference between the colliding beams, the nucleon–nucleon center-of-mass in the pPb collisions is not at rest with respect to the laboratory frame. Massless particles emitted at $\eta_{\text{cm}} = 0$ in the nucleon–nucleon center-of-mass frame will be detected at $\eta = -0.465$ (clockwise proton beam) or 0.465 (counterclockwise proton beam) in the laboratory frame. A sample of 2.76 TeV PbPb data collected during the 2011 LHC heavy-ion run, corresponding to an integrated luminosity of 2.3 μb^{-1}, is also analyzed for comparison purposes.

Minimum bias (MB) pPb events were triggered by requiring at least one track with $p_T > 0.4$ GeV/c to be found in the pixel tracker for a pPb bunch crossing. Because of hardware limits on the data acquisition rate, only a small fraction ($\sim 10^{-3}$) of all minimum bias triggered events were recorded (i.e., the trigger was "prescaled"). In order to select high-multiplicity pPb collisions, a dedicated high-multiplicity trigger was implemented using the CMS level-1 (L1) and high-level trigger (HLT) systems. At L1, the total transverse energy summed over ECAL and HCAL was required to be greater than a given threshold (20 or 40 GeV). Online track reconstruction for the HLT was based on the three layers of pixel detectors, and required a track origin within a cylindrical region of length 30 cm along the beam and radius 0.2 cm perpendicular to the beam. For each event, the vertex reconstructed with the highest number of pixel tracks was selected. The number of pixel tracks ($N_{\text{trk}}^{\text{online}}$) with $|\eta| < 2.4$, $p_T > 0.4$ GeV/c, and a distance of closest approach of 0.4 cm or less to this vertex, was determined for each event. Data were taken with thresholds of $N_{\text{trk}}^{\text{online}} > 100, 130$ (L1 threshold of 20 GeV), and 160, 190 (L1 threshold of 40 GeV) with prescaling factors dependent on the instantaneous luminosity. The $N_{\text{trk}}^{\text{online}} > 190$ trigger was never prescaled throughout the entire run.

In the offline analysis, hadronic collisions were selected by requiring a coincidence of at least one HF calorimeter tower with more than 3 GeV of total energy in each of the HF detectors. Events were also required to contain at least one reconstructed primary vertex within 15 cm of the nominal interaction point along the beam axis and within 0.15 cm transverse to the beam trajectory. At least two reconstructed tracks were required to be associated with the primary vertex. Beam related background was suppressed by rejecting events for which less than 25% of all reconstructed tracks were of good quality (i.e., the tracks selected for physics analysis as will be discussed later).

The pPb instantaneous luminosity provided by the LHC in the 2013 run resulted in approximately 3% probability of at least one additional interaction occurring in the same bunch crossing, resulting in pileup events. A procedure for rejecting pileup events was developed to select clean, single-vertex pPb collisions. The approach was to investigate the number of tracks, $N_{\text{trk}}^{\text{best}}$ that is assigned to the best reconstructed vertex (e.g., the one with the greatest number of associated tracks), and $N_{\text{trk}}^{\text{add}}$ assigned to each

of the additional vertices, as well as the distance between the two vertices in the z direction ($\Delta z_{\rm vtx}$). Based on studies using low pileup pPb data (from the 2012 pilot run), PbPb data, and MC simulations, events with $N_{\rm trk}^{\rm add}$ above a certain threshold at a given $\Delta z_{\rm vtx}$ were identified as pileup events and removed from the event sample. This threshold was set to be higher for smaller $\Delta z_{\rm vtx}$ and larger $N_{\rm trk}^{\rm best}$ to account for the fact that events with a smaller vertex separation and greater multiplicity have a higher probability of vertex splitting in the reconstruction algorithm. The residual pileup fraction was estimated to be no more than 0.2% for the highest multiplicity pPb interactions studied in this Letter.

Among those pPb interactions simulated with the [52] and HIJING [53] event generators, which have at least one primary particle with total energy $E > 3$ GeV in both η ranges of $-5 < \eta < -3$ and $3 < \eta < 5$, the above criteria are found to select 97–98% of the events.

In this analysis, the CMS *highPurity* [54] tracks were used. Additionally, a reconstructed track was only considered as a primary track candidate if the significance of the separation along the beam axis (z) between the track and the best vertex, $d_z/\sigma(d_z)$, and the significance of the impact parameter relative to the best vertex transverse to the beam, $d_{\rm T}/\sigma(d_{\rm T})$, were each less than 3. The relative uncertainty of the transverse momentum measurement, $\sigma(p_{\rm T})/p_{\rm T}$, was required to be less than 10%. To ensure high tracking efficiency and reduce the rate of misidentified tracks, only tracks within $|\eta| < 2.4$ and with $p_{\rm T} > 0.3$ GeV/c were used in the analysis (a different $p_{\rm T}$ cutoff of 0.4 GeV/c used in multiplicity determination due to constraint of online processing time at HLT).

The events were divided into classes of reconstructed track multiplicity, $N_{\rm trk}^{\rm offline}$, where primary tracks with $|\eta| < 2.4$ and $p_{\rm T} > 0.4$ GeV/c were counted, in a method similar to the approach used in Refs. [38,39]. Data from the HLT minimum bias trigger were used for $N_{\rm trk}^{\rm offline} < 120$, while the track multiplicity triggers with online track thresholds of 100, 130, 160, and 190 were used for $120 \leqslant N_{\rm trk}^{\rm offline} < 150$, $150 \leqslant N_{\rm trk}^{\rm offline} < 185$, $185 \leqslant N_{\rm trk}^{\rm offline} < 220$, and $N_{\rm trk}^{\rm offline} \geqslant 220$, respectively. This correspondence ensures at least 90% trigger efficiency in each multiplicity bin. The fractions of MB triggered events after event selections falling into each of the main multiplicity classes are listed in Table 1. The table also lists the average values of $N_{\rm trk}^{\rm offline}$ and $N_{\rm trk}^{\rm corrected}$, the event multiplicity of charged particles with $|\eta| < 2.4$ and $p_{\rm T} > 0.4$ GeV/c corrected for detector acceptance and efficiency of the track reconstruction algorithm, as discussed in the following section. The average $N_{\rm trk}^{\rm offline}$ values for MB pPb samples with opposite proton beam directions are found to be consistent within 0.2%.

In order to compare directly the pPb and PbPb systems using event selections based on the multiplicity of the collisions, a subset of data from peripheral PbPb collisions collected during the 2011 LHC heavy-ion run with a minimum bias trigger were reanalyzed using the same track reconstruction algorithm as the one employed for pp and pPb collisions. The selection of events and tracks is the same as for the present pPb analysis although a different trigger is used. A description of the 2011 PbPb data can be found in Ref. [55]. The average $N_{\rm trk}^{\rm offline}$ and $N_{\rm trk}^{\rm corrected}$ values, and corresponding average PbPb collision centrality, as determined by the total energy deposited in the HF calorimeters [9], are listed in Table 1 for each $N_{\rm trk}^{\rm offline}$ bin.

4. Analysis technique

4.1. Two-particle correlation function

The two-particle correlation functions are constructed following the procedure established in Refs. [33,34,39]. For each track multiplicity class, "trigger" particles are defined as primary charged tracks within a given $p_{\rm T}^{\rm trig}$ range. The number of trigger particles in the event is denoted by $N_{\rm trig}$. Particle pairs are formed by associating each trigger particle with the remaining charged primary particles from a specified $p_{\rm T}^{\rm assoc}$ interval (which can be either the same or different from the $p_{\rm T}^{\rm trig}$ range). The per-trigger-particle associated yield is defined as

$$\frac{1}{N_{\rm trig}}\frac{{\rm d}^2N^{\rm pair}}{{\rm d}\Delta\eta\,{\rm d}\Delta\phi} = B(0,0)\times\frac{S(\Delta\eta,\Delta\phi)}{B(\Delta\eta,\Delta\phi)}, \tag{1}$$

where $\Delta\eta$ and $\Delta\phi$ are the differences in η and ϕ of the pair. The signal pair distribution, $S(\Delta\eta,\Delta\phi)$, represents the yield of particle pairs normalized by $N_{\rm trig}$ from the same event,

$$S(\Delta\eta,\Delta\phi) = \frac{1}{N_{\rm trig}}\frac{{\rm d}^2N^{\rm same}}{{\rm d}\Delta\eta\,{\rm d}\Delta\phi}. \tag{2}$$

The mixed-event pair distribution,

$$B(\Delta\eta,\Delta\phi) = \frac{1}{N_{\rm trig}}\frac{{\rm d}^2N^{\rm mix}}{{\rm d}\Delta\eta\,{\rm d}\Delta\phi}, \tag{3}$$

is constructed by pairing the trigger particles in each event with the associated particles from 10 different random events in the same 2 cm wide $z_{\rm vtx}$ range and from the same track multiplicity class. Here, $N^{\rm mix}$ denotes the number of pairs taken from the mixed events. The ratio $B(0,0)/B(\Delta\eta,\Delta\phi)$ accounts for the random combinatorial background as well as for pair-acceptance effects, with $B(0,0)$ representing the mixed-event associated yield for both particles of the pair going in approximately the same direction and thus having full pair-acceptance (with a bin width of 0.3 in $\Delta\eta$ and $\pi/16$ in $\Delta\phi$). The signal and background distributions are first calculated for each event, and then averaged over all the events within the track multiplicity class. The range of $0 < |\Delta\eta| < 4.8$ and $0 < |\Delta\phi| < \pi$ is used to fill one quadrant of the $(\Delta\eta,\Delta\phi)$ histograms, with the other three quadrants filled (for illustration purposes) by reflection to cover a $(\Delta\eta,\Delta\phi)$ range of $-4.8 < \Delta\eta < 4.8$ and $-\pi/2 < \Delta\phi < 3\pi/2$ for the 2D correlation functions, as will be shown later in Fig. 2.

4.2. Azimuthal anisotropy harmonics from two- and four-particle correlations

The azimuthal anisotropy harmonics are determined from a Fourier decomposition of long-range two-particle $\Delta\phi$ correlation functions,

$$\frac{1}{N_{\rm trig}}\frac{{\rm d}N^{\rm pair}}{{\rm d}\Delta\phi} = \frac{N_{\rm assoc}}{2\pi}\left[1+\sum_n 2V_{n\Delta}\cos(n\Delta\phi)\right], \tag{4}$$

as described in Refs. [33,34], where $V_{n\Delta}$ are the Fourier coefficients and $N_{\rm assoc}$ represents the total number of pairs per trigger particle for a given $(p_{\rm T}^{\rm trig}, p_{\rm T}^{\rm assoc})$ bin. The first three Fourier terms are included in the fits to the dihadron correlation functions. Including additional terms has a negligible effect on the results of the Fourier fit. A minimum $|\Delta\eta|$ of 2 units is applied to remove short-range correlations from jet fragmentation. The elliptic and triangular anisotropy harmonics, $v_2\{2,|\Delta\eta|>2\}$ and $v_3\{2,|\Delta\eta|>2\}$, from the two-particle correlation method can be extracted as a function of $p_{\rm T}$ from the fitted Fourier coefficients,

$$v_n\{2,|\Delta\eta|>2\}(p_{\rm T}) = \frac{V_{n\Delta}(p_{\rm T},p_{\rm T}^{\rm ref})}{\sqrt{V_{n\Delta}(p_{\rm T}^{\rm ref},p_{\rm T}^{\rm ref})}}, \quad n=2,3. \tag{5}$$

Here, a fixed $p_{\rm T}^{\rm ref}$ range for the "reference particles" is chosen to be $0.3 < p_{\rm T} < 3.0$ GeV/c.

Table 1
Fraction of MB triggered events after event selections in each multiplicity bin, and the average multiplicity of reconstructed tracks per bin with $|\eta| < 2.4$ and $p_T > 0.4$ GeV/c, before ($N_{trk}^{offline}$) and after ($N_{trk}^{corrected}$) efficiency correction, for 2.76 TeV PbPb and 5.02 TeV pPb data.

$N_{trk}^{offline}$ bin	PbPb data			pPb data		
	⟨Centrality⟩ ± RMS (%)	$\langle N_{trk}^{offline}\rangle$	$\langle N_{trk}^{corrected}\rangle$	Fraction	$\langle N_{trk}^{offline}\rangle$	$\langle N_{trk}^{corrected}\rangle$
$[0, \infty)$				1.00	40	50 ± 2
$[0, 20)$	92 ± 4	10	13 ± 1	0.31	10	12 ± 1
$[20, 30)$	86 ± 4	24	30 ± 1	0.14	25	30 ± 1
$[30, 40)$	83 ± 4	34	43 ± 2	0.12	35	42 ± 2
$[40, 50)$	80 ± 4	44	55 ± 2	0.10	45	54 ± 2
$[50, 60)$	78 ± 3	54	68 ± 3	0.09	54	66 ± 3
$[60, 80)$	75 ± 3	69	87 ± 4	0.12	69	84 ± 4
$[80, 100)$	72 ± 3	89	112 ± 5	0.07	89	108 ± 5
$[100, 120)$	70 ± 3	109	137 ± 6	0.03	109	132 ± 6
$[120, 150)$	67 ± 3	134	168 ± 7	0.02	132	159 ± 7
$[150, 185)$	64 ± 3	167	210 ± 9	4×10^{-3}	162	195 ± 9
$[185, 220)$	62 ± 2	202	253 ± 11	5×10^{-4}	196	236 ± 10
$[220, 260)$	59 ± 2	239	299 ± 13	6×10^{-5}	232	280 ± 12
$[260, 300)$	57 ± 2	279	350 ± 15	3×10^{-6}	271	328 ± 14
$[300, 350)$	55 ± 2	324	405 ± 18	1×10^{-7}	311	374 ± 16

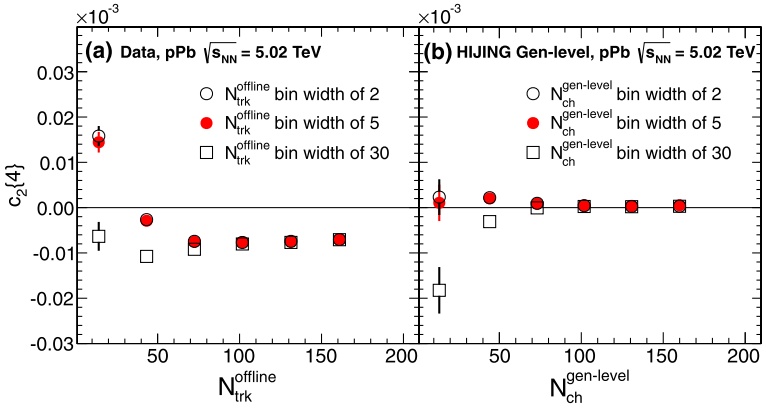

Fig. 1. The $c_2\{4\}$ values as a function of multiplicity calculated for bin width of 30 (open squares), and first derived using a smaller bin width of 2 (open circles) or 5 (solid circles) and then averaging over the same wider bin of 30, for pPb data (a) and HIJING MC simulations (b) at $\sqrt{s_{NN}} = 5.02$ TeV.

The second-order elliptic harmonic, $v_2\{4\}$, is also determined from a four-particle cumulant analysis using the Q-cumulant method described in Ref. [48]. A reference flow $v_2\{4\}$ is first determined by correlating four particles within the tracker acceptance $|\eta| < 2.4$ and in a p_T^{ref} range, $0.3 < p_T^{ref} < 3.0$ GeV/c,

$$v_2^{ref}\{4\} = \sqrt[4]{-c_2\{4\}}, \tag{6}$$

where the reference four-particle cumulant, $c_2\{4\}$, is calculated as,

$$c_2\{4\} = \left\langle\left\langle e^{-2i(\phi_1+\phi_2-\phi_3-\phi_4)}\right\rangle\right\rangle - 2 \times \left\langle\left\langle e^{-2i(\phi_1-\phi_2)}\right\rangle\right\rangle^2. \tag{7}$$

Here, ϕ_1, ϕ_2, ϕ_3, ϕ_4 are the azimuthal angles of four different particles in an event, and $\langle\langle\cdot\rangle\rangle$ represents the average over all particles from all events within a given multiplicity range.

With respect to the reference flow, the differential $v_2\{4\}(p_T)$ as a function of p_T is then derived via

$$v_2\{4\}(p_T) = \frac{-d_2\{4\}(p_T)}{(v_2^{ref}\{4\})^3}, \tag{8}$$

where the differential four-particle cumulant, $d_2\{4\}(p_T)$, is calculated by replacing one of the four reference particles in Eq. (7) by a particle from a particular p_T region. An $\Delta\eta$ requirement is not applied in the four-particle cumulant analysis since short-range two-particle correlations are inherently minimized by applying this multi-particle method.

4.3. Corrections and systematic uncertainties

In performing the correlation analyses, each reconstructed track is weighted by a correction factor, described in Refs. [33,34]. This factor accounts for the reconstruction efficiency, the detector acceptance, and the fraction of misreconstructed tracks. Detailed studies of tracking performance based on MC simulations and collision data can be found in Ref. [56]. The combined geometrical acceptance and efficiency for track reconstruction exceeds 60% for $p_T \approx 0.3$ GeV/c and $|\eta| < 2.4$. The efficiency is greater than 90% in the $|\eta| < 1$ region for $p_T > 0.6$ GeV/c. For the entire multiplicity range (up to $N_{trk}^{offline} \sim 350$) studied in this Letter, no dependence of the tracking efficiency on multiplicity is found and the rate of misreconstructed tracks remains at the 1–2% level.

Based on the studies in Ref. [56], the total uncertainty of the absolute tracking efficiency is estimated to be 3.9%. This translates directly into a 3.9% systematic uncertainty of the extracted associated yields, while the v_n values are insensitive to it. Systematic uncertainties due to track quality requirements are examined by varying the track selections for $d_z/\sigma(d_z)$ and $d_{xy}/\sigma(d_{xy})$ from 2 to 5. The results of both associated yields and v_n are found to be insensitive to these track selections within 2%. A comparison of high-multiplicity pPb data for a given multiplicity range but collected by two different HLT triggers with different trigger efficiencies shows an agreement within 1%. Possible contamination of residual pileup events is also investigated. By varying the

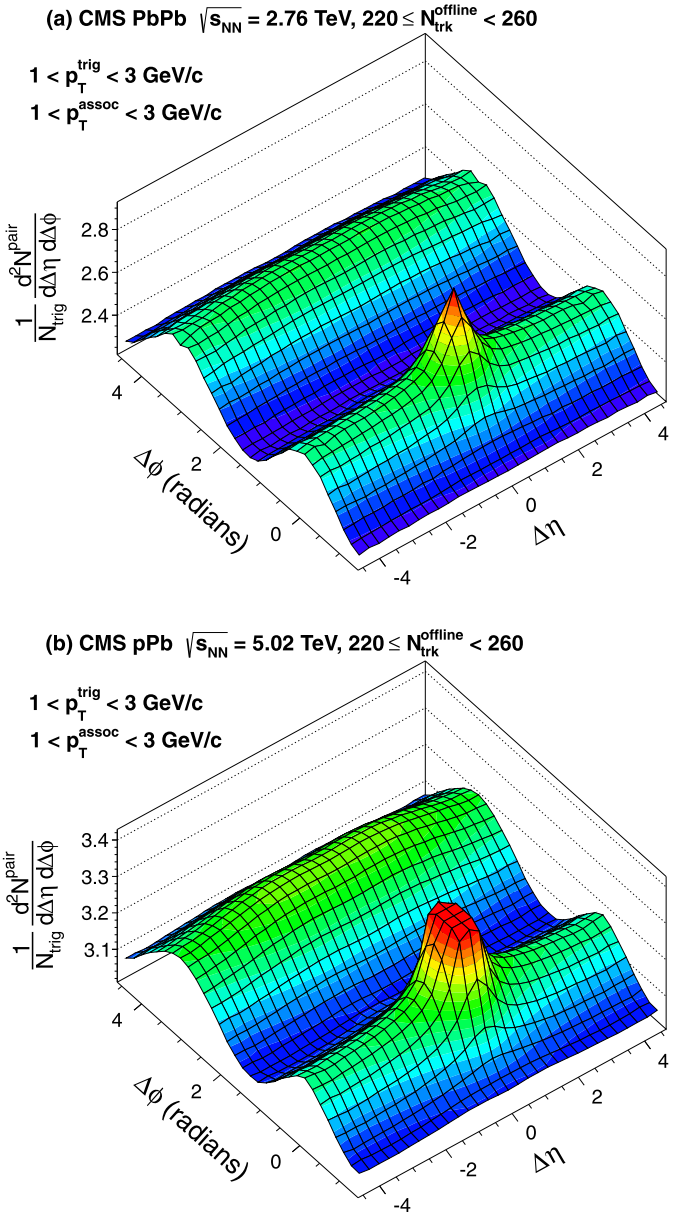

Fig. 2. The 2D two-particle correlation functions for (a) 2.76 TeV PbPb and (b) 5.02 TeV pPb collisions for pairs of charged particles with $1 < p_T^{trig} < 3$ GeV/c and $1 < p_T^{assoc} < 3$ GeV/c within the $220 \leqslant N_{trk}^{offline} < 260$ multiplicity bin. The sharp near-side peak from jet correlations is truncated to emphasize the structure outside that region.

z_{vtx} range in performing the analysis, the pileup probability is expected to vary by a factor of 3–4. The systematic uncertainties for associated yields and v_n from possible residual pileup effects are estimated to be 1–2% for $N_{trk}^{offline} < 200$, increasing to 6% for $N_{trk}^{offline} \geqslant 260$.

The event-by-event variation of track multiplicity within a given multiplicity bin width is found to have an effect on the four-particle cumulant analysis, especially for the low-multiplicity region. The $c_2\{4\}$ values calculated directly for a multiplicity bin width of 30 show a large discrepancy from those derived first using a smaller bin width (e.g., 2 or 5) and then averaged over the same wider bin, as illustrated for pPb data in Fig. 1(a) and for pPb MC HIJING simulation (generator level only) in Fig. 1(b). The event multiplicity in HIJING, $N_{ch}^{gen\text{-}level}$, is counted for charged primary particles at the generator level with $|\eta| < 2.4$ and $p_T > 0.4$ GeV/c. With smaller multiplicity bin widths, the $c_2\{4\}$ values for HIJING are largely consistent with zero. This is expected due to the absence of collective effect in the HIJING event generator. An $N_{trk}^{offline}$ bin width of 5 is chosen for the $v_2\{4\}$ analysis in this Letter. Studies performed with different $N_{trk}^{offline}$ bin widths, allowing different multiplicity content in the bins, suggest a systematic uncertainty of only 1% for $N_{trk}^{offline} > 100$ but up to 10% for the low-multiplicity region $N_{trk}^{offline} < 60$.

The different systematic sources described above are added in quadrature to obtain the overall systematic uncertainty, shown as boxes in Figs. 5–11.

5. Results

5.1. Correlation functions

Fig. 2 shows the 2D two-particle correlation functions measured in 2.76 TeV PbPb (a) and 5.02 TeV pPb (b) collisions, for pairs of charged particles with $1 < p_T^{trig} < 3$ GeV/c and $1 < p_T^{assoc} < 3$ GeV/c, and with the track multiplicity in the range $220 \leqslant N_{trk}^{offline} < 260$. For PbPb collisions, this $N_{trk}^{offline}$ range corresponds to an average centrality of approximately 60%, as shown in Table 1. For both high-multiplicity systems, in addition to the correlation peak near $(\Delta\eta, \Delta\phi) = (0, 0)$ due to jet fragmentation (truncated for better illustration of the full correlation structure), a pronounced long-range structure is seen at $\Delta\phi \approx 0$ extending at least 4.8 units in $|\Delta\eta|$. This structure was previously observed in high-multiplicity ($N_{trk}^{offline} \sim 110$) pp collisions at $\sqrt{s} = 7$ TeV [38] and pPb collisions at $\sqrt{s_{NN}} = 5.02$ TeV [39–41]. The structure is also prominent in AA collisions over a wide range of energies [2,12–15,33,34,36,37]. On the away side ($\Delta\phi \approx \pi$) of the correlation functions, a long-range structure is also seen and found to exhibit a magnitude similar to that on the near side for this p_T range. In non-central AA collisions, this $\cos(2\Delta\phi)$-like azimuthal correlation structure is believed to arise primarily from elliptic flow [31]. However, the away-side correlations must also contain contributions from back-to-back jets, which need to be accounted for before extracting any other source of correlations.

To investigate the observed correlations in finer detail and to obtain a quantitative comparison of the structure in the pp, pPb, and PbPb systems, one-dimensional (1D) distributions in $\Delta\phi$ are found by averaging the signal and background 2D distributions over $|\Delta\eta| < 1$ (defined as the "short-range region") and $|\Delta\eta| > 2$ (defined as the "long-range region") respectively, as done in Refs. [33,34,38,39]. The correlated portion of the associated yield is estimated using an implementation of the zero-yield-at-minimum (ZYAM) procedure [57]. In this procedure, the 1D $\Delta\phi$ correlation function is first fitted by a second-order polynomial in the region $0.1 < |\Delta\phi| < 2$. The minimum value of the polynomial, C_{ZYAM}, is then subtracted from the 1D $\Delta\phi$ correlation function as a constant background (containing no information about correlations) such that its minimum is shifted to have zero associated yield. The statistical uncertainty in the minimum level obtained by the ZYAM procedure, combined with the deviations arising from the choice of fit range in $|\Delta\phi|$, gives an absolute uncertainty of ± 0.003 in the associated event-normalized yield that is independent of multiplicity and p_T.

Figs. 3 and 4 show the 1D $\Delta\phi$ correlation functions, after applying the ZYAM procedure, for PbPb and pPb data, respectively, in the multiplicity range $N_{trk}^{offline} < 20$ (open) and $220 \leqslant N_{trk}^{offline} < 260$ (filled). Various selections of p_T^{trig} are shown for a fixed p_T^{assoc} range of 1–2 GeV/c in both the long-range (top) and short-range (bottom) regions, with p_T increasing from left to right. The curves show the Fourier fits from Eq. (4), which will be discussed in detail

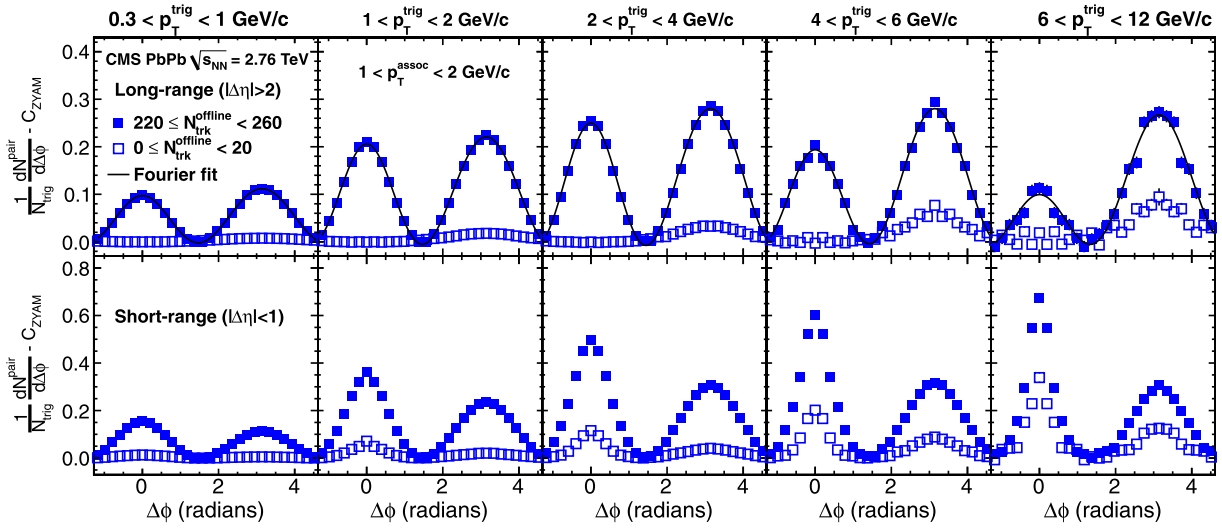

Fig. 3. The 1D two-particle correlation functions for 2.76 TeV PbPb collisions within the multiplicity range $220 \leqslant N_{\mathrm{trk}}^{\mathrm{offline}} < 260$ (filled squares) and $N_{\mathrm{trk}}^{\mathrm{offline}} < 20$ (open squares), for pairs of charged particles with fixed $p_{\mathrm{T}}^{\mathrm{assoc}}$1–2 GeV/$c$ in five $p_{\mathrm{T}}^{\mathrm{trig}}$ ranges, in the long-range region ($|\Delta\eta| > 2$, top) and in the short-range region ($|\Delta\eta| < 1$, bottom). The curves on the top panels correspond to the Fourier fits from Eq. (4) including the first three terms.

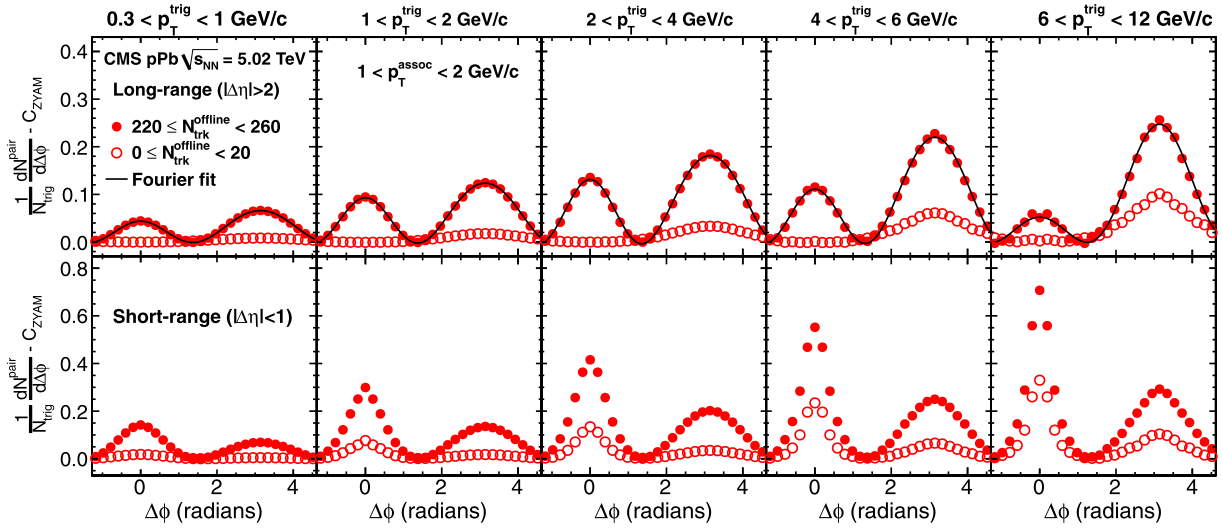

Fig. 4. The 1D two-particle correlation functions for 5.02 TeV pPb collisions under the same conditions as in Fig. 3.

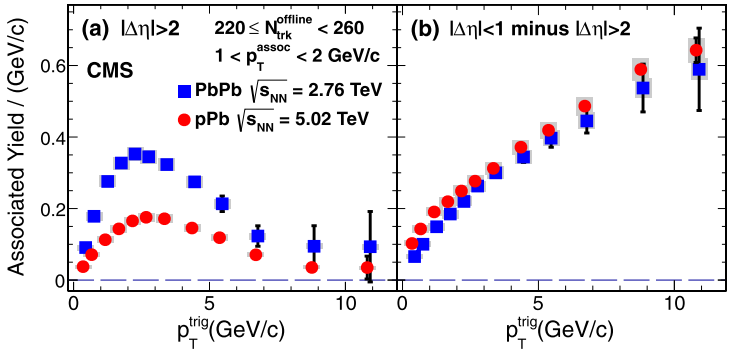

Fig. 5. Associated event-normalized yield for the near-side correlation function integrated over the region $|\Delta\phi| < 1.2$, averaged over the (a) long-range ($|\Delta\eta| > 2$) region and (b) short-range ($|\Delta\eta| < 1$) region, from which the event-normalized yield of the long-range region is subtracted. The results are shown as a function of $p_{\mathrm{T}}^{\mathrm{trig}}$ at $1 < p_{\mathrm{T}}^{\mathrm{assoc}} < 2$ GeV/c for events with $220 \leqslant N_{\mathrm{trk}}^{\mathrm{offline}} < 260$ for 5.02 TeV pPb collisions (filled circles) and 2.76 TeV PbPb collisions (filled squares). The error bars correspond to statistical uncertainties, while the shaded areas denote the systematic uncertainties.

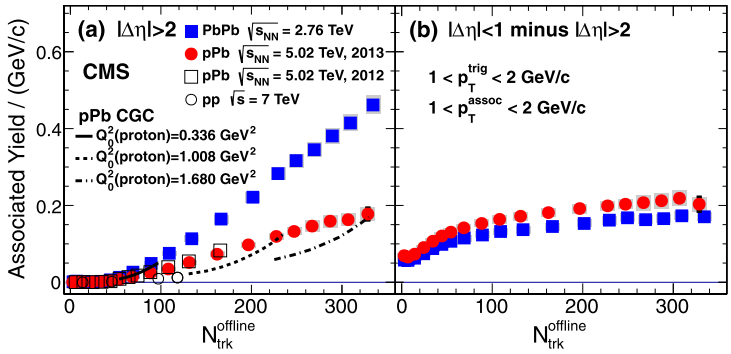

Fig. 6. Associated event-normalized yields for the near-side correlation function as a function of multiplicity $N_{\mathrm{trk}}^{\mathrm{offline}}$ for $1 < p_{\mathrm{T}}^{\mathrm{trig}} < 2$ GeV/c and $1 < p_{\mathrm{T}}^{\mathrm{assoc}} < 2$ GeV/c under the same conditions as in Fig. 5. The results for 7 TeV pp collisions (open circles) [38] and 5.02 TeV pPb collisions from 2012 run (open squares) [34], as well as calculations from the Color Glass Condensate (CGC) theory (curves) [58], are also shown.

later. The pPb and PbPb yields show a similar correlation structure and a similar evolution of this structure with $p_{\mathrm{T}}^{\mathrm{trig}}$ over a wide range of $p_{\mathrm{T}}^{\mathrm{trig}}$. As illustrated in Fig. 2, while the near-side long-range signal varies only by a small amount over almost 5 units in $\Delta\eta$, the short-range region shows a strong $\Delta\eta$ dependence. Therefore, the $\Delta\phi$ correlation functions in the short-range region of Figs. 3 and 4 reflect the contributions of both jet fragmentation and long-range correlations. For $N_{\mathrm{trk}}^{\mathrm{offline}} < 20$, no near-side correlations are observed in the long-range region of either pPb or PbPb data.

5.2. Integrated associated yields

The strength of the near-side correlations for short- and long-range regions can be further quantified by integrating the event-normalized associated yield from Figs. 3 and 4 over $|\Delta\phi| < 1.2$. The resulting integrated yields are shown for pPb and PbPb in Fig. 5 as a function of $p_{\mathrm{T}}^{\mathrm{trig}}$ for $1 < p_{\mathrm{T}}^{\mathrm{assoc}} < 2$ GeV/c and $220 \leqslant N_{\mathrm{trk}}^{\mathrm{offline}} < 260$, and in Fig. 6 as a function of $N_{\mathrm{trk}}^{\mathrm{offline}}$ for $1 < p_{\mathrm{T}}^{\mathrm{trig}} < 2$ GeV/c and $1 < p_{\mathrm{T}}^{\mathrm{assoc}} < 2$ GeV/c together with the pp results from Ref. [38]. The "jet yield" is extracted by subtracting the event-normalized integrated yield in the long-range region from that in the short-range region. The error bars correspond to statistical uncertainties, while the shaded boxes indicate the systematic uncertainties discussed in Section 4.3.

The jet yield (Fig. 5(b)) increases with $p_{\mathrm{T}}^{\mathrm{trig}}$ in both pPb and PbPb as would be expected if higher energy jets, which fragment into more final-state particles, are selected by requiring higher-$p_{\mathrm{T}}^{\mathrm{trig}}$ particles. In striking contrast to the jet yields, the $p_{\mathrm{T}}^{\mathrm{trig}}$ dependence of the long-range yields (Fig. 5(a)) show an initial rise, reaching a maximum at $p_{\mathrm{T}} \approx 2$–3 GeV/c, followed by a falloff with values consistent with zero for $p_{\mathrm{T}}^{\mathrm{trig}} \sim 12$ GeV/c.

The jet yield (shown in Fig. 6(b)) as a function of multiplicity increases by a factor of two as $N_{\mathrm{trk}}^{\mathrm{offline}}$ increases from 0 to 60. It then rises moderately by 20–30%, for $60 \leqslant N_{\mathrm{trk}}^{\mathrm{offline}} < 350$, the limit of this measurement. This demonstrates that by selecting high-track-multiplicity PbPb and pPb events, there is no significant bias to stronger jet-like correlations (at least for the p_{T} range of 1–2 GeV/c). It was previously observed in Ref. [39] that the long-range yield as a function of multiplicity only becomes significant at $N_{\mathrm{trk}}^{\mathrm{offline}} \sim 40$–$50$, followed by a monotonic rise with $N_{\mathrm{trk}}^{\mathrm{offline}}$ in pp and pPb collisions. In this Letter, the measurement of the long-range yield (Fig. 6(a)) in pPb collisions is extended to a significantly wider multiplicity range. A direct comparison to the pp [38] and PbPb collision systems is also provided. The PbPb long-range yield is found to become significant for $N_{\mathrm{trk}}^{\mathrm{offline}} \gtrsim 40$–$50$, similar to the pp and pPb results. For both pPb and PbPb data, the long-range yields continue increasing with multiplicity up to $N_{\mathrm{trk}}^{\mathrm{offline}} \sim 350$. The long-range yield in PbPb is about a factor of two larger than in pPb, and a factor of eight larger than in pp at a given multiplicity and $p_{\mathrm{T}}^{\mathrm{trig}}$ value. In contrast to the weak multiplicity dependence of jet-like correlations shown in Fig. 6(b) at higher values of $N_{\mathrm{trk}}^{\mathrm{offline}}$, a monotonic increase of the magnitude of the long-range yield with the overall event multiplicity is observed in all three collision systems.

In the framework of the color glass condensate model, the long-range correlation structure in pPb collisions has been attributed to initial-state gluon correlations, where the contribution of collimated gluon emissions is significantly enhanced in the gluon saturation regime [44,45,58]. This model qualitatively describes the increase in the long-range yield for higher-multiplicity events as shown in Fig. 6(a), where three different initial proton saturation scales are assumed for the pPb system. Since the calculations depend on saturation scales for both protons and lead nuclei, the data provide valuable constraints on the multiplicity dependence of these parameters in the model.

5.3. Fourier harmonics v_n

Long-range correlations in pPb collisions have also been predicted in hydrodynamic models [46] where a collective hydrodynamic expansion of the system with fluctuating initial conditions is assumed. To compare with hydrodynamic predictions of the long-range correlations in pPb collisions, the elliptic (v_2) and triangular (v_3) flow harmonics are extracted from a Fourier decomposition of 1D $\Delta\phi$ correlation functions, $v_2\{2, |\Delta\eta| > 2\}$ and $v_3\{2, |\Delta\eta| > 2\}$, for the long-range region ($|\Delta\eta| > 2$) as shown in Figs. 7 and 8, respectively. To further reduce the residual nonflow correlations on the away side, a four-particle cumulant analysis is also used to extract the elliptic flow, $v_2\{4\}$, as shown in Fig. 7. As mentioned in Section 1, the multi-particle correlation technique has the advantage of suppressing short-range jet-like correlations compared to two-particle correlations. It thus provides a cleaner measurement of the long-range correlations of collective nature involving many particles from the system.

As seen in Fig. 7, the magnitude of the v_2 signal is found to be larger in PbPb than in pPb by about 30% for $p_{\mathrm{T}} < 2$ GeV/c (the near-side long-range yield is related to v_2^2 as suggested in Eq. (4), and thus differs by a larger factor between the two systems as shown in Fig. 6). The difference between the $v_2\{2, |\Delta\eta| > 2\}$ and $v_2\{4\}$ results could be, a consequence of event-by-event fluctuations in the flow signal or nonflow correlations, as believed to be the case in PbPb collisions [59]. The $v_3\{2, |\Delta\eta| > 2\}$ component, shown in Fig. 8, reaches the same maximum value for the two systems but has a much smaller magnitude than $v_2\{2, |\Delta\eta| > 2\}$

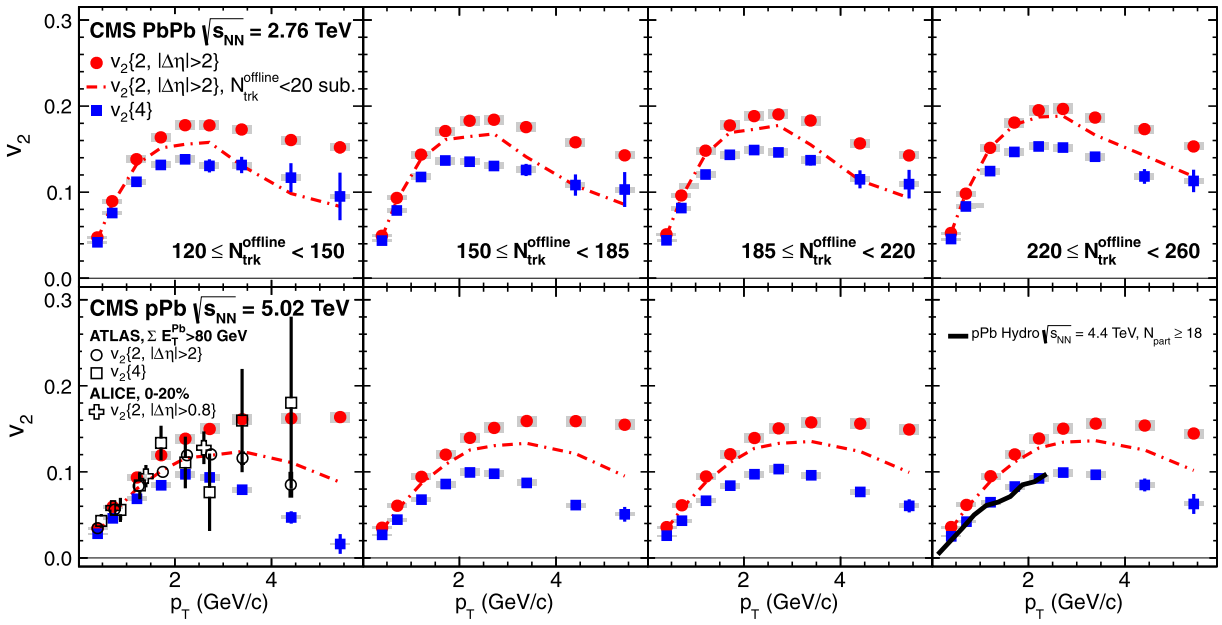

Fig. 7. The differential $v_2\{2, |\Delta\eta| > 2\}$ (filled circles) and $v_2\{4\}$ (filled squares) values for four multiplicity ranges obtained with $|\eta| < 2.4$ and a p_T^{ref} range of 0.3–3 GeV/c. The results are for 2.76 TeV PbPb collisions (top) and for 5.02 TeV pPb collisions (bottom). The error bars correspond to statistical uncertainties, while the shaded areas denote the systematic uncertainties. Results after subtracting the low-multiplicity data ($N_{\text{trk}}^{\text{offline}} < 20$) as well as predictions from a hydrodynamic model are also shown (curves). The open markers show the results from ALICE [40] and ATLAS [49] using 2012 pPb data.

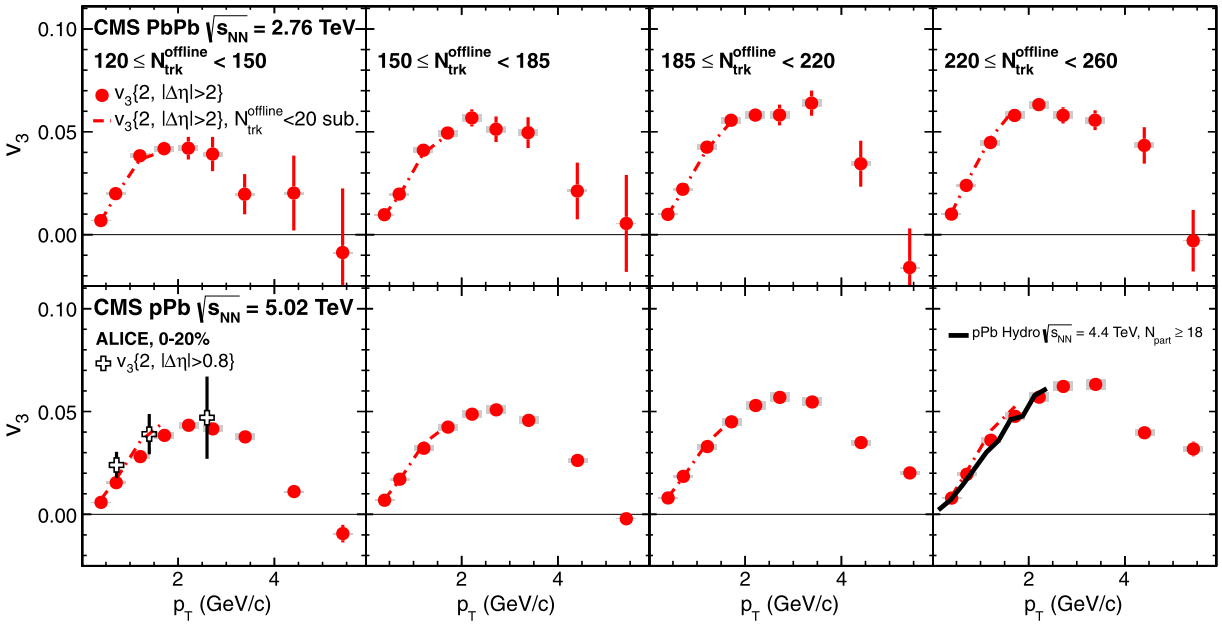

Fig. 8. The differential $v_3\{2, |\Delta\eta| > 2\}$ values for four multiplicity ranges under the same conditions as in Fig. 7.

over the entire p_T range investigated here. The p_T dependencies of both the v_2 and v_3 coefficients are similar, with peak values at 2–3 GeV/c range for PbPb and slightly higher for pPb. The elliptic and triangular flow components predicted by the hydrodynamic calculation of Ref. [46] for pPb collisions at $\sqrt{s_{NN}} = 4.4$ TeV and for $p_T < 2.5$ GeV/c are also shown, and compared to the high-multiplicity pPb data in Figs. 7 and 8. The calculations have little collision energy dependence, and assume the number of participating nucleons to be larger or equal to 18, approximately corresponding to the top 4% central pPb events. However, contributions from event-by-event fluctuations of the flow signal around its average value are not accounted for in the calculations. Therefore, the v_2 calculated in Ref. [46] is expected to lie between the values from the two- and four-particle correlation methods [59]. Detailed studies of v_2 using various techniques in PbPb collisions at $\sqrt{s_{NN}} = 2.76$ TeV by CMS can be found in Ref. [9].

As mentioned above, the residual jet-like correlations on the away side of the two-particle correlation function could contribute to the extracted $v_n\{2, |\Delta\eta| > 2\}$ signal, and thus induce a systematic uncertainty in the quantitative comparison to hydrodynamic calculations. Assuming that the jet-induced correlations are invariant with event multiplicity in pPb collisions, the ALICE [40] and ATLAS [41] experiments proposed to subtract the results of low-multiplicity events, where the long-range correlation signal is not

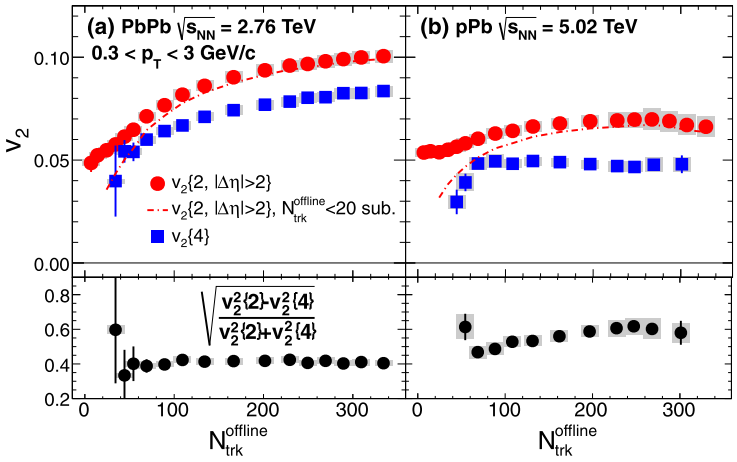

Fig. 9. Top: the $v_2\{2, |\Delta\eta| > 2\}$ (circles) and $v_2\{4\}$ (squares) values as a function of $N_{trk}^{offline}$ for $0.3 < p_T < 3$ GeV/c, in 2.76 TeV PbPb collisions (a) and 5.02 TeV pPb collisions (b). Bottom: upper limits on the relative v_2 fluctuations estimated from $v_2\{2\}$ and $v_2\{4\}$ in 2.76 TeV PbPb collisions (a) and 5.02 TeV pPb collisions (b). The error bars correspond to statistical uncertainties, while the shaded areas denote the systematic uncertainties. Results after subtracting the low-multiplicity data ($N_{trk}^{offline} < 20$) are also shown (curves).

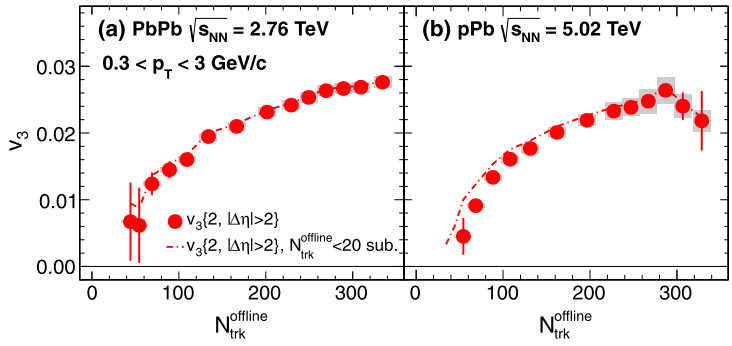

Fig. 10. The $v_3\{2, |\Delta\eta| > 2\}$ values as a function of $N_{trk}^{offline}$ for $0.3 < p_T < 3$ GeV/c, in 2.76 TeV PbPb collisions (a) and 5.02 TeV pPb collisions (b). The error bars correspond to statistical uncertainties, while the shaded areas denote the systematic uncertainties.

present, from those of high-multiplicity events. While further justification of this assumption is still required, a similar procedure is applied in this Letter for comparison purposes. The Fourier coefficients, $V_{n\Delta}$, extracted from Eq. (4) for $N_{trk}^{offline} < 20$ (corresponding to the 70–100% lowest-multiplicity events for pPb) are subtracted from the data in the higher-multiplicity region:

$$V_{n\Delta}^{sub} = V_{n\Delta} - V_{n\Delta}\left(N_{trk}^{offline} < 20\right) \times \frac{N_{assoc}(N_{trk}^{offline} < 20)}{N_{assoc}} \times \frac{Y_{jet}}{Y_{jet}(N_{trk}^{offline} < 20)}, \quad (9)$$

where Y_{jet} represents the near-side jet yield. The ratio, $Y_{jet}/Y_{jet}(N_{trk}^{offline} < 20)$, is introduced to account for the enhanced jet correlations due to the selection of higher-multiplicity events seen in Fig. 6(b). This procedure is tested using the HIJING model, where there are no final-state interactions of jets in pPb collisions. The residual $V_{n\Delta}^{sub}$ in HIJING after subtraction is found to be less than 5%. The low-multiplicity-subtracted $v_2\{2, |\Delta\eta| > 2\}$ and $v_3\{2, |\Delta\eta| > 2\}$ (limited to $p_T < 2$ GeV/c for v_3 due to the low statistical precision of the low-multiplicity data) are shown as dash-dotted curves in Figs. 7 and 8. After applying the subtraction procedure, the results at low p_T remain almost unchanged, while a reduction is seen in v_2 for higher p_T particles. This is consistent with the observation of stronger jet-like correlations at higher p_T in Fig. 5(b). The CMS data are compared to the measurement by the ATLAS experiment for an event multiplicity class (selected based on the total transverse energy measured with $3.1 < \eta < 4.9$ in the direction of the Pb beam) comparable to $120 \leqslant N_{trk}^{offline} < 150$ used in the CMS analysis, after subtracting the 50–100% lowest-multiplicity data. The $v_2\{2\}$ and $v_3\{2\}$ data measured by the ALICE experiment for the 0–20% highest-multiplicity pPb collisions [40] are also shown in Figs. 7 and 8. Results from all three experiments are consistent within quoted uncertainties.

The multiplicity dependencies of v_2 and v_3 for PbPb and pPb collisions, averaged over the p_T range from 0.3 to 3 GeV/c, are shown in Figs. 9 and 10, respectively. The $v_2\{2, |\Delta\eta| > 2\}$ and $v_2\{4\}$ values in PbPb collisions exhibit a moderate increase with $N_{trk}^{offline}$, while these coefficients remain relatively constant as a function of multiplicity for pPb data at larger values of $N_{trk}^{offline}$. This is consistent with the monotonic rise of the associated yield as a function of multiplicity shown in Fig. 6, which is mainly driven by the increase of total number of pairs per trigger particle, as indicated in Eq. (4). Similarly to Figs. 7 and 8, the PbPb data show a larger v_2 signal than observed for the pPb data over a wide multiplicity range, while the magnitude of $v_3\{2, |\Delta\eta| > 2\}$ is remarkably similar for both systems at the same event multiplicity. This similarity of the triangular flow is not trivially expected within a hydrodynamic picture since the initial-state collision geometry is very different for the pPb and PbPb systems. Below an $N_{trk}^{offline}$ value of 40–50, neither $v_3\{2, |\Delta\eta| > 2\}$ nor $v_2\{4\}$ could be reliably extracted. The loss of a $v_2\{4\}$ signal indicates either the absence of collective effects for very-low-multiplicity collisions, or the breakdown of the four-particle cumulant technique in the limit of a small number of particles. The procedure of subtracting the low-multiplicity data to attempt to remove jet correlations

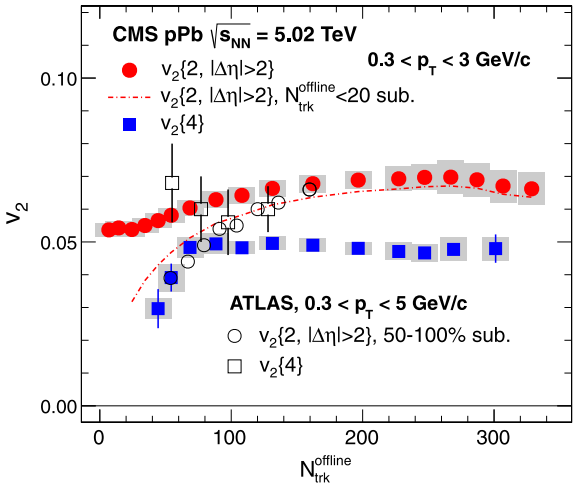

Fig. 11. The $v_2\{2, |\Delta\eta| > 2\}$ and $v_2\{4\}$ values as a function of $N_{\rm trk}^{\rm offline}$ for $0.3 < p_{\rm T} < 3$ GeV/c, measured by CMS in 5.02 TeV pPb collisions (filled). The dash-dotted curve shows the CMS $v_2\{2, |\Delta\eta| > 2\}$ values after subtracting the 70–100% lowest-multiplicity data, to be compared with the ATLAS results subtracted by 50–100% lowest-multiplicity data (open) [49]. The error bars correspond to statistical uncertainties, while the shaded areas denote the systematic uncertainties.

is also performed here and shown as dash-dotted curves in Figs. 9 and 10. The $v_3\{2, |\Delta\eta| > 2\}$ values become larger after subtraction, especially for the low-multiplicity region, due to the fact that $V_{3\Delta}$ extracted for $N_{\rm trk}^{\rm offline} < 20$ is negative. The resulting $v_2\{2, |\Delta\eta| > 2\}$ and $v_3\{2, |\Delta\eta| > 2\}$ are found to remain almost unchanged after subtraction in the high-multiplicity region (i.e., for $N_{\rm trk}^{\rm offline} > 200$). This is expected since, for a given associated yield from jet correlations, the contribution to $v_n\{2\}$ is suppressed by $1/\sqrt{N_{\rm trk}^{\rm offline}}$ as the multiplicity increases, as indicated by Eq. (4). Therefore, the higher-multiplicity events provide a much cleaner environment for studying the long-range correlations.

Fig. 11 shows the comparison of $v_2\{2, |\Delta\eta| > 2\}$ and $v_2\{4\}$ results as a function of multiplicity from CMS, averaged over $0.3 < p_{\rm T} < 3$ GeV/c, with those obtained by the ATLAS experiment, averaged over $0.3 < p_{\rm T} < 5$ GeV/c with the data from the 2012 pPb run. The ATLAS $v_2\{2, |\Delta\eta| > 2\}$ values have the contribution from the 50–100% lowest-multiplicity data subtracted, while the corresponding CMS data, shown as a curve in Fig. 11, use the 70–100% lowest-multiplicity events for the subtraction. The difference in the low-multiplicity events used for the subtraction could explain the slight discrepancy in the resulting $v_2\{2, |\Delta\eta| > 2\}$ data from the two experiments. The $v_2\{4\}$ values from ATLAS are systematically higher than the CMS data. This may be accounted for by the multiplicity fluctuation effect discussed previously (e.g., Fig. 1), although the discrepancy is not large with respect to the uncertainties.

Finally, the magnitude of event-by-event v_2 fluctuations is estimated from the difference in the $v_2\{2, |\Delta\eta| > 2\}$ and $v_2\{4\}$ results. If hydrodynamic flow is the dominant source of the correlations, the relative v_2 fluctuations can be approximated by $\sqrt{(v_2^2\{2\} - v_2^2\{4\})/(v_2^2\{2\} + v_2^2\{4\})}$ [59]. The resulting flow fluctuation values calculated for pPb and PbPb collisions are shown in the bottom two panels of Fig. 9, with 40% v_2 fluctuations observed in PbPb and 50–60% fluctuations in pPb collisions. This magnitude of v_2 fluctuations in 2.76 TeV PbPb collisions at the LHC is comparable to the value measured in 200 GeV AuAu collisions at RHIC [60]. As a consequence of possible residual nonflow correlations from back-to-back jets on the away side in the $v_2\{2, |\Delta\eta| > 2\}$ measurement, these results should be considered as upper limits on the flow fluctuations.

6. Summary

Detailed studies of two- and four-particle azimuthal correlations have been performed in pPb collisions at $\sqrt{s_{NN}} = 5.02$ TeV by the CMS experiment. The new measurements extend previous CMS two-particle correlation analyses in pPb collisions to a significantly broader particle multiplicity range. A direct comparison of the correlation data between pPb and PbPb collisions was presented as a function of particle multiplicity and transverse momentum. The observed correlations were quantified in terms of the integrated near-side associated yields and azimuthal anisotropy Fourier harmonics (v_n). For both pPb and PbPb collisions, elliptic (v_2) and triangular (v_3) flow Fourier harmonics were extracted from long-range two-particle correlations. Furthermore, the elliptic flow was studied with a four-particle cumulant analysis, where multi-particle correlations can be directly investigated.

For a fixed $p_{\rm T}^{\rm assoc}$ range, the long-range yield and anisotropy harmonics show similar trends as a function of $p_{\rm T}^{\rm trig}$, first increasing and then decreasing with a maximum at $p_{\rm T}^{\rm trig} \approx 2$–3 GeV/$c$ in both pPb and PbPb collisions. For pPb collisions, the long-range associated yield rises monotonically with particle multiplicity. Correspondingly, the v_2 harmonics obtained from the two- and four-particle correlation analyses show only a weak multiplicity dependence. Comparing the pPb and PbPb systems at the same multiplicity and $p_{\rm T}$, the long-range yield and v_2 signals are found to have a larger magnitude in PbPb than in pPb, while the v_3 signal has a remarkably similar magnitude in both systems. In addition, the long-range yield, v_2 obtained from the four-particle method, and v_3 all become apparent at about the same multiplicity. The comprehensive correlation data presented in this Letter, spanning a very wide range in particle multiplicity and transverse momentum, should provide significant insights into the origin of the azimuthal correlations in small collision systems, particularly in the context of the hydrodynamic and color glass condensate models.

Acknowledgements

We congratulate our colleagues in the CERN accelerator departments for the excellent performance of the LHC and thank the technical and administrative staffs at CERN and at other CMS institutes for their contributions to the success of the CMS effort. In addition, we gratefully acknowledge the computing centres and personnel of the Worldwide LHC Computing Grid for delivering so effectively the computing infrastructure essential to our analyses. Finally, we acknowledge the enduring support for the construction and operation of the LHC and the CMS detector provided by the following funding agencies: BMWF and FWF (Austria); FNRS and FWO (Belgium); CNPq, CAPES, FAPERJ, and FAPESP (Brazil); MEYS (Bulgaria); CERN; CAS, MoST, and NSFC (China); COLCIENCIAS (Colombia); MSES (Croatia); RPF (Cyprus); MoER, SF0690030s09 and ERDF (Estonia); Academy of Finland, MEC, and HIP (Finland); CEA and CNRS/IN2P3 (France); BMBF, DFG, and HGF (Germany); GSRT (Greece); OTKA and NKTH (Hungary); DAE and DST (India); IPM (Iran); SFI (Ireland); INFN (Italy); NRF and WCU (Republic of Korea); LAS (Lithuania); CINVESTAV, CONACYT, SEP, and UASLP-FAI (Mexico); MSI (New Zealand); PAEC (Pakistan); MSHE and NSC (Poland); FCT (Portugal); JINR (Armenia, Belarus, Georgia, Ukraine, Uzbekistan); MON, RosAtom, RAS and RFBR (Russia); MSTD (Serbia); SEIDI and CPAN (Spain); Swiss Funding Agencies (Switzerland); NSC (Taipei); ThEPCenter, IPST and NSTDA (Thailand); TUBITAK and TAEK (Turkey); NASU (Ukraine); STFC (United Kingdom); DOE and NSF (USA).

Individuals have received support from the Marie-Curie programme and the European Research Council and EPLANET (European Union); the Leventis Foundation; the A.P. Sloan Foundation; the Alexander von Humboldt Foundation; the Belgian Federal Science Policy Office; the Fonds pour la Formation à la Recherche dans l'Industrie et dans l'Agriculture (FRIA-Belgium); the Agentschap voor Innovatie door Wetenschap en Technologie (IWT-Belgium); the Ministry of Education, Youth and Sports (MEYS) of Czech Republic; the Council of Science and Industrial Research, India; the Compagnia di San Paolo (Torino); the HOMING PLUS programme of Foundation for Polish Science, cofinanced by EU, Regional Development Fund; and the Thalis and Aristeia programmes cofinanced by EU-ESF and the Greek NSRF.

Open access

References

[1] J.-Y. Ollitrault, Anisotropy as a signature of transverse collective flow, Phys. Rev. D 46 (1992) 229, http://dx.doi.org/10.1103/PhysRevD.46.229.
[2] B. Alver, et al., PHOBOS Collaboration, System size dependence of cluster properties from two- particle angular correlations in Cu + Cu and Au + Au collisions at $\sqrt{s_{NN}} = 200$ GeV, Phys. Rev. C 81 (2010) 024904, http://dx.doi.org/10.1103/PhysRevC.81.024904, arXiv:0812.1172.
[3] K. Adcox, et al., PHENIX Collaboration, Formation of dense partonic matter in relativistic nucleus nucleus collisions at RHIC: Experimental evaluation by the PHENIX Collaboration, Nucl. Phys. A 757 (2005) 184, http://dx.doi.org/10.1016/j.nuclphysa.2005.03.086, arXiv:nucl-ex/0410003.
[4] J. Adams, et al., STAR Collaboration, Experimental and theoretical challenges in the search for the quark gluon plasma: The STAR Collaboration's critical assessment of the evidence from RHIC collisions, Nucl. Phys. A 757 (2005) 102, http://dx.doi.org/10.1016/j.nuclphysa.2005.03.085, arXiv:nucl-ex/0501009.
[5] B.B. Back, et al., The PHOBOS perspective on discoveries at RHIC, Nucl. Phys. A 757 (2005) 28, http://dx.doi.org/10.1016/j.nuclphysa.2005.03.084, arXiv:nucl-ex/0410022.
[6] S.S. Adler, et al., PHENIX Collaboration, Saturation of azimuthal anisotropy in Au + Au collisions at $\sqrt{s_{NN}} = 62$ GeV to 200 GeV, Phys. Rev. Lett. 94 (2005) 232302, http://dx.doi.org/10.1103/PhysRevLett.94.232302.
[7] G. Agakishiev, et al., STAR Collaboration, Directed and elliptic flow of charged particles in Cu + Cu collisions at $\sqrt{s_{NN}} = 22.4$ GeV, Phys. Rev. C 85 (2012) 014901, http://dx.doi.org/10.1103/PhysRevC.85.014901.
[8] B. Alver, et al., PHOBOS Collaboration, System size, energy, pseudorapidity, and centrality dependence of elliptic flow, Phys. Rev. Lett. 98 (2007) 242302, http://dx.doi.org/10.1103/PhysRevLett.98.242302.
[9] CMS Collaboration, Measurement of the elliptic anisotropy of charged particles produced in PbPb collisions at nucleon–nucleon center-of-mass energy = 2.76 TeV, Phys. Rev. C 87 (2013) 014902, http://dx.doi.org/10.1103/PhysRevC.87.014902, arXiv:1204.1409.
[10] ALICE Collaboration, Elliptic flow of charged particles in pb–pb collisions at $\sqrt{s_{NN}} = 2.76$ TeV, Phys. Rev. Lett. 105 (2010) 252302, http://dx.doi.org/10.1103/PhysRevLett.105.252302.
[11] G. Aad, et al., ATLAS Collaboration, Measurement of the pseudorapidity and transverse momentum dependence of the elliptic flow of charged particles in lead–lead collisions at $\sqrt{s_{NN}} = 2.76$ TeV with the ATLAS detector, Phys. Lett. B 707 (2012) 330, http://dx.doi.org/10.1016/j.physletb.2011.12.056, arXiv:1108.6018.
[12] J. Adams, et al., STAR Collaboration, Distributions of charged hadrons associated with high transverse momentum particles in pp and Au + Au collisions at $\sqrt{s_{NN}} = 200$ GeV, Phys. Rev. Lett. 95 (2005) 152301, http://dx.doi.org/10.1103/PhysRevLett.95.152301, arXiv:nucl-ex/0501016.
[13] B.I. Abelev, et al., STAR Collaboration, Long range rapidity correlations and jet production in high energy nuclear collisions, Phys. Rev. C 80 (2009) 064912, http://dx.doi.org/10.1103/PhysRevC.80.064912, arXiv:0909.0191.
[14] B. Alver, et al., PHOBOS Collaboration, High transverse momentum triggered correlations over a large pseudorapidity acceptance in Au + Au collisions at $\sqrt{s_{NN}} = 200$ GeV, Phys. Rev. Lett. 104 (2010) 062301, http://dx.doi.org/10.1103/PhysRevLett.104.062301, arXiv:0903.2811.
[15] B.I. Abelev, et al., STAR Collaboration, Three-particle coincidence of the long range pseudorapidity correlation in high energy nucleus–nucleus collisions, Phys. Rev. Lett. 105 (2010) 022301, http://dx.doi.org/10.1103/PhysRevLett.105.022301, arXiv:0912.3977.
[16] N. Armesto, C.A. Salgado, U.A. Wiedemann, Measuring the collective flow with jets, Phys. Rev. Lett. 93 (2004) 242301, http://dx.doi.org/10.1103/PhysRevLett.93.242301, arXiv:hep-ph/0405301.
[17] A. Majumder, B. Muller, S.A. Bass, Longitudinal broadening of quenched jets in turbulent color fields, Phys. Rev. Lett. 99 (2007) 042301, http://dx.doi.org/10.1103/PhysRevLett.99.042301, arXiv:hep-ph/0611135.
[18] C.B. Chiu, R.C. Hwa, Pedestal and peak structure in jet correlation, Phys. Rev. C 72 (2005) 034903, http://dx.doi.org/10.1103/PhysRevC.72.034903, arXiv:nucl-th/0505014.
[19] C.-Y. Wong, Momentum kick model description of the near-side ridge and jet quenching, Phys. Rev. C 78 (2008) 064905, http://dx.doi.org/10.1103/PhysRevC.78.064905, arXiv:0806.2154.
[20] P. Romatschke, Momentum broadening in an anisotropic plasma, Phys. Rev. C 75 (2007) 014901, http://dx.doi.org/10.1103/PhysRevC.75.014901, arXiv:hep-ph/0607327.
[21] E.V. Shuryak, On the origin of the "ridge" phenomenon induced by jets in heavy ion collisions, Phys. Rev. C 76 (2007) 047901, http://dx.doi.org/10.1103/PhysRevC.76.047901, arXiv:0706.3531.
[22] S.A. Voloshin, Two particle rapidity, transverse momentum, and azimuthal correlations in relativistic nuclear collisions and transverse radial expansion, Nucl. Phys. A 749 (2005) 287, http://dx.doi.org/10.1016/j.nuclphysa.2004.12.053, arXiv:nucl-th/0410024.
[23] A.P. Mishra, R.K. Mohapatra, P.S. Saumia, A.M. Srivastava, Superhorizon fluctuations and acoustic oscillations in relativistic heavy-ion collisions, Phys. Rev. C 77 (2008) 064902, http://dx.doi.org/10.1103/PhysRevC.77.064902, arXiv:0711.1323.
[24] J. Takahashi, et al., Topology studies of hydrodynamics using two particle correlation analysis, Phys. Rev. Lett. 103 (2009) 242301, http://dx.doi.org/10.1103/PhysRevLett.103.242301, arXiv:0902.4870.
[25] B. Alver, G. Roland, Collision geometry fluctuations and triangular flow in heavy-ion collisions, Phys. Rev. C 81 (2010) 054905, http://dx.doi.org/10.1103/PhysRevC.81.054905, arXiv:1003.0194;
B. Alver, G. Roland, Phys. Rev. C 81 (2010) 054905, http://dx.doi.org/10.1103/PhysRevC.82.039903, Erratum.
[26] B.H. Alver, C. Gombeaud, M. Luzum, J.-Y. Ollitrault, Triangular flow in hydrodynamics and transport theory, Phys. Rev. C 82 (2010) 034913, http://dx.doi.org/10.1103/PhysRevC.82.034913, arXiv:1007.5469.
[27] B. Schenke, S. Jeon, C. Gale, Elliptic and triangular flow in event-by-event $D = 3 + 1$ viscous hydrodynamics, Phys. Rev. Lett. 106 (2011) 042301, http://dx.doi.org/10.1103/PhysRevLett.106.042301, arXiv:1009.3244.
[28] H. Petersen, G.-Y. Qin, S.A. Bass, B. Müller, Triangular flow in event-by-event ideal hydrodynamics in Au + Au collisions at $\sqrt{s_{NN}} = 200$ GeV, Phys. Rev. C 82 (2010) 041901, http://dx.doi.org/10.1103/PhysRevC.82.041901, arXiv:1008.0625.
[29] J. Xu, C.M. Ko, Effects of triangular flow on di-hadron azimuthal correlations in relativistic heavy ion collisions, Phys. Rev. C 83 (2011) 021903, http://dx.doi.org/10.1103/PhysRevC.83.021903, arXiv:1011.3750.
[30] D. Teaney, L. Yan, Triangularity and dipole asymmetry in heavy ion collisions, Phys. Rev. C 83 (2011) 064904, http://dx.doi.org/10.1103/PhysRevC.83.064904, arXiv:1010.1876.
[31] S. Voloshin, Y. Zhang, Flow study in relativistic nuclear collisions by Fourier expansion of azimuthal particle distributions, Z. Phys. C 70 (1996) 665, http://dx.doi.org/10.1007/s002880050141, arXiv:hep-ph/9407282.
[32] Z. Qiu, C. Shen, U. Heinz, Hydrodynamic elliptic and triangular flow in Pb–Pb collisions at $\sqrt{s_{NN}} = 2.76$ TeV, Phys. Lett. B 707 (2012) 151, http://dx.doi.org/10.1016/j.physletb.2011.12.041, arXiv:1110.3033.
[33] CMS Collaboration, Long-range and short-range dihadron angular correlations in central PbPb collisions at a nucleon–nucleon center of mass energy of 2.76 TeV, JHEP 1107 (2011) 076, http://dx.doi.org/10.1007/JHEP07(2011)076, arXiv:1105.2438.
[34] CMS Collaboration, Centrality dependence of dihadron correlations and azimuthal anisotropy harmonics in PbPb collisions at $\sqrt{s_{NN}} = 2.76$ TeV, Eur. Phys. J. C 72 (2012) 2012, http://dx.doi.org/10.1140/epjc/s10052-012-2012-3, arXiv:1201.3158.
[35] ALICE Collaboration, Higher harmonic anisotropic flow measurements of charged particles in Pb–Pb collisions at $\sqrt{s_{NN}} = 2.76$ TeV, Phys. Rev. Lett. 107 (2011) 032301, http://dx.doi.org/10.1103/PhysRevLett.107.032301, arXiv:1105.3865.
[36] ALICE Collaboration, Harmonic decomposition of two-particle angular correlations in Pb–Pb collisions at $\sqrt{s_{NN}} = 2.76$ TeV, Phys. Lett. B 708 (2012) 249, http://dx.doi.org/10.1016/j.physletb.2012.01.060, arXiv:1109.2501.
[37] ATLAS Collaboration, Measurement of the azimuthal anisotropy for charged particle production in $\sqrt{s_{NN}} = 2.76$ TeV lead–lead collisions with the ATLAS detector, Phys. Rev. C 86 (2012) 014907, http://dx.doi.org/10.1103/PhysRevC.86.014907, arXiv:1203.3087.

[38] CMS Collaboration, Observation of long-range near-side angular correlations in proton–proton collisions at the LHC, JHEP 1009 (2010) 091, http://dx.doi.org/10.1007/JHEP09(2010)091, arXiv:1009.4122.
[39] CMS Collaboration, Observation of long-range near-side angular correlations in proton–lead collisions at the LHC, Phys. Lett. B 718 (2013) 795, http://dx.doi.org/10.1016/j.physletb.2012.11.025, arXiv:1210.5482.
[40] ALICE Collaboration, Long-range angular correlations on the near and away side in pPb collisions at $\sqrt{s_{NN}} = 5.02$ TeV, Phys. Lett. B 719 (2013) 29, http://dx.doi.org/10.1016/j.physletb.2013.01.012, arXiv:1212.2001.
[41] ATLAS Collaboration, Observation of associated near-side and away-side long-range correlations in $\sqrt{s_{NN}} = 5.02$ TeV proton–lead collisions with the ATLAS detector, Phys. Rev. Lett. 110 (2013) 182302, http://dx.doi.org/10.1103/PhysRevLett.110.182302, arXiv:1212.5198.
[42] A. Adare, et al., PHENIX Collaboration, Quadrupole anisotropy in dihadron azimuthal correlations in central d + Au collisions at $\sqrt{s_{NN}} = 200$ GeV, arXiv:1303.1794, Phys. Rev. Lett. (2013), submitted for publication.
[43] W. Li, Observation of a 'Ridge' correlation structure in high multiplicity proton–proton collisions: A brief review, Mod. Phys. Lett. A 27 (2012) 1230018, http://dx.doi.org/10.1142/S0217732312300182, arXiv:1206.0148.
[44] K. Dusling, R. Venugopalan, Evidence for BFKL and saturation dynamics from dihadron spectra at the LHC, Phys. Rev. D 87 (2013) 051502, http://dx.doi.org/10.1103/PhysRevD.87.051502, arXiv:1210.3890.
[45] K. Dusling, R. Venugopalan, Explanation of systematics of CMS p + Pb high multiplicity dihadron data at $\sqrt{s_{NN}} = 5.02$ TeV, Phys. Rev. D 87 (2013) 054014, http://dx.doi.org/10.1103/PhysRevD.87.054014, arXiv:1211.3701.
[46] P. Bozek, Collective flow in p–Pb and d–Pd collisions at TeV energies, Phys. Rev. C 85 (2012) 014911, http://dx.doi.org/10.1103/PhysRevC.85.014911, arXiv:1112.0915.
[47] P. Bozek, W. Broniowski, Correlations from hydrodynamic flow in pPb collisions, Phys. Lett. B 718 (2013) 1557, http://dx.doi.org/10.1016/j.physletb.2012.12.051, arXiv:1211.0845.
[48] A. Bilandzic, R. Snellings, S. Voloshin, Flow analysis with cumulants: Direct calculations, Phys. Rev. C 83 (2011) 044913, http://dx.doi.org/10.1103/PhysRevC.83.044913, arXiv:1010.0233.
[49] ATLAS Collaboration, Measurement with the ATLAS detector of multi-particle azimuthal correlations in p + Pb collisions at $\sqrt{s_{NN}} = 5.02$ TeV, arXiv:1303.2084, Phys. Lett. B (2013), submitted for publication.
[50] CMS Collaboration, The CMS experiment at the CERN LHC, JINST 3 (2008) S08004, http://dx.doi.org/10.1088/1748-0221/3/08/S08004.
[51] S. Agostinelli, et al., Geant4 Collaboration, Geant4—A simulation toolkit, Nucl. Instrum. and Meth. A 506 (2003) 250, http://dx.doi.org/10.1016/S0168-9002(03)01368-8.
[52] S. Porteboeuf, T. Pierog, K. Werner, Producing hard processes regarding the complete event: The EPOS event generator, arXiv:1006.2967, 2010.
[53] M. Gyulassy, X.-N. Wang, HIJING 1.0: A Monte Carlo program for parton and particle production in high-energy hadronic and nuclear collisions, Comput. Phys. Commun. 83 (1994) 307, http://dx.doi.org/10.1016/0010-4655(94)90057-4, arXiv:nucl-th/9502021.
[54] CMS Collaboration, Tracking and vertexing results from first collisions, CMS Physics Analysis Summary CMS-PAS-TRK-10-001, http://cdsweb.cern.ch/record/1258204, 2010.
[55] CMS Collaboration, Azimuthal anisotropy of charged particles at high transverse momenta in PbPb collisions at $\sqrt{s_{NN}} = 2.76$ TeV, Phys. Rev. Lett. 109 (2012) 022301, http://dx.doi.org/10.1103/PhysRevLett.109.022301, arXiv:1204.1850.
[56] CMS Collaboration, Measurement of tracking efficiency, CMS Physics Analysis Summary, CMS-PAS-TRK-10–002, http://cdsweb.cern.ch/record/1279139, 2010.
[57] N.N. Ajitanand, J.M. Alexander, P. Chung, W.G. Holzmann, M. Issah, R.A. Lacey, A. Shevel, A. Taranenko, P. Danielewicz, Decomposition of harmonic and jet contributions to particle-pair correlations at ultrarelativistic energies, Phys. Rev. C 72 (2005) 011902, http://dx.doi.org/10.1103/PhysRevC.72.011902, arXiv:nucl-ex/0501025.
[58] K. Dusling, R. Venugopalan, Comparison of the color glass condensate to dihadron correlations in proton–proton and proton–nucleus collisions, arXiv:1302.7018, 2013.
[59] J.-Y. Ollitrault, A.M. Poskanzer, S.A. Voloshin, Effect of flow fluctuations and nonflow on elliptic flow methods, Phys. Rev. C 80 (2009) 014904, http://dx.doi.org/10.1103/PhysRevC.80.014904, arXiv:0904.2315.
[60] B. Alver, et al., PHOBOS Collaboration, Event-by-event fluctuations of azimuthal particle anisotropy in Au + Au Collisions at $\sqrt{s_{NN}} = 200$ GeV, Phys. Rev. Lett. 104 (2010) 142301, http://dx.doi.org/10.1103/PhysRevLett.104.142301, arXiv:nucl-ex/0702036.

CMS Collaboration

S. Chatrchyan, V. Khachatryan, A.M. Sirunyan, A. Tumasyan

Yerevan Physics Institute, Yerevan, Armenia

W. Adam, T. Bergauer, M. Dragicevic, J. Erö, C. Fabjan [1], M. Friedl, R. Frühwirth [1], V.M. Ghete, N. Hörmann, J. Hrubec, M. Jeitler [1], W. Kiesenhofer, V. Knünz, M. Krammer [1], I. Krätschmer, D. Liko, I. Mikulec, D. Rabady [2], B. Rahbaran, C. Rohringer, H. Rohringer, R. Schöfbeck, J. Strauss, A. Taurok, W. Treberer-Treberspurg, W. Waltenberger, C.-E. Wulz [1]

Institut für Hochenergiephysik der OeAW, Wien, Austria

V. Mossolov, N. Shumeiko, J. Suarez Gonzalez

National Centre for Particle and High Energy Physics, Minsk, Belarus

S. Alderweireldt, M. Bansal, S. Bansal, T. Cornelis, E.A. De Wolf, X. Janssen, A. Knutsson, S. Luyckx, L. Mucibello, S. Ochesanu, B. Roland, R. Rougny, Z. Staykova, H. Van Haevermaet, P. Van Mechelen, N. Van Remortel, A. Van Spilbeeck

Universiteit Antwerpen, Antwerpen, Belgium

F. Blekman, S. Blyweert, J. D'Hondt, A. Kalogeropoulos, J. Keaveney, M. Maes, A. Olbrechts, S. Tavernier, W. Van Doninck, P. Van Mulders, G.P. Van Onsem, I. Villella

Vrije Universiteit Brussel, Brussel, Belgium

B. Clerbaux, G. De Lentdecker, L. Favart, A.P.R. Gay, T. Hreus, A. Léonard, P.E. Marage, A. Mohammadi, L. Perniè, T. Reis, T. Seva, L. Thomas, C. Vander Velde, P. Vanlaer, J. Wang

Université Libre de Bruxelles, Bruxelles, Belgium

V. Adler, K. Beernaert, L. Benucci, A. Cimmino, S. Costantini, S. Dildick, G. Garcia, B. Klein, J. Lellouch, A. Marinov, J. Mccartin, A.A. Ocampo Rios, D. Ryckbosch, M. Sigamani, N. Strobbe, F. Thyssen, M. Tytgat, S. Walsh, E. Yazgan, N. Zaganidis

Ghent University, Ghent, Belgium

S. Basegmez, C. Beluffi [3], G. Bruno, R. Castello, A. Caudron, L. Ceard, C. Delaere, T. du Pree, D. Favart, L. Forthomme, A. Giammanco [4], J. Hollar, P. Jez, V. Lemaitre, J. Liao, O. Militaru, C. Nuttens, D. Pagano, A. Pin, K. Piotrzkowski, A. Popov [5], M. Selvaggi, J.M. Vizan Garcia

Université Catholique de Louvain, Louvain-la-Neuve, Belgium

N. Beliy, T. Caebergs, E. Daubie, G.H. Hammad

Université de Mons, Mons, Belgium

G.A. Alves, M. Correa Martins Junior, T. Martins, M.E. Pol, M.H.G. Souza

Centro Brasileiro de Pesquisas Fisicas, Rio de Janeiro, Brazil

W.L. Aldá Júnior, W. Carvalho, J. Chinellato [6], A. Custódio, E.M. Da Costa, D. De Jesus Damiao, C. De Oliveira Martins, S. Fonseca De Souza, H. Malbouisson, M. Malek, D. Matos Figueiredo, L. Mundim, H. Nogima, W.L. Prado Da Silva, A. Santoro, A. Sznajder, E.J. Tonelli Manganote [6], A. Vilela Pereira

Universidade do Estado do Rio de Janeiro, Rio de Janeiro, Brazil

C.A. Bernardes [b], F.A. Dias [a,7], T.R. Fernandez Perez Tomei [a], E.M. Gregores [b], C. Lagana [a], P.G. Mercadante [b], S.F. Novaes [a], Sandra S. Padula [a]

[a] *Universidade Estadual Paulista, São Paulo, Brazil*
[b] *Universidade Federal do ABC, São Paulo, Brazil*

V. Genchev [2], P. Iaydjiev [2], S. Piperov, M. Rodozov, G. Sultanov, M. Vutova

Institute for Nuclear Research and Nuclear Energy, Sofia, Bulgaria

A. Dimitrov, R. Hadjiiska, V. Kozhuharov, L. Litov, B. Pavlov, P. Petkov

University of Sofia, Sofia, Bulgaria

J.G. Bian, G.M. Chen, H.S. Chen, C.H. Jiang, D. Liang, S. Liang, X. Meng, J. Tao, J. Wang, X. Wang, Z. Wang, H. Xiao, M. Xu

Institute of High Energy Physics, Beijing, China

C. Asawatangtrakuldee, Y. Ban, Y. Guo, W. Li, S. Liu, Y. Mao, S.J. Qian, H. Teng, D. Wang, L. Zhang, W. Zou

State Key Laboratory of Nuclear Physics and Technology, Peking University, Beijing, China

C. Avila, C.A. Carrillo Montoya, L.F. Chaparro Sierra, J.P. Gomez, B. Gomez Moreno, J.C. Sanabria

Universidad de Los Andes, Bogota, Colombia

N. Godinovic, D. Lelas, R. Plestina [8], D. Polic, I. Puljak

Technical University of Split, Split, Croatia

Z. Antunovic, M. Kovac

University of Split, Split, Croatia

V. Brigljevic, S. Duric, K. Kadija, J. Luetic, D. Mekterovic, S. Morovic, L. Tikvica

Institute Rudjer Boskovic, Zagreb, Croatia

A. Attikis, G. Mavromanolakis, J. Mousa, C. Nicolaou, F. Ptochos, P.A. Razis

University of Cyprus, Nicosia, Cyprus

M. Finger, M. Finger Jr.

Charles University, Prague, Czech Republic

Y. Assran [9], S. Elgammal [10], A. Ellithi Kamel [11], M.A. Mahmoud [12], A. Mahrous [13], A. Radi [14,15]

Academy of Scientific Research and Technology of the Arab Republic of Egypt, Egyptian Network of High Energy Physics, Cairo, Egypt

M. Kadastik, M. Müntel, M. Murumaa, M. Raidal, L. Rebane, A. Tiko

National Institute of Chemical Physics and Biophysics, Tallinn, Estonia

P. Eerola, G. Fedi, M. Voutilainen

Department of Physics, University of Helsinki, Helsinki, Finland

J. Härkönen, V. Karimäki, R. Kinnunen, M.J. Kortelainen, T. Lampén, K. Lassila-Perini, S. Lehti, T. Lindén, P. Luukka, T. Mäenpää, T. Peltola, E. Tuominen, J. Tuominiemi, E. Tuovinen, L. Wendland

Helsinki Institute of Physics, Helsinki, Finland

T. Tuuva

Lappeenranta University of Technology, Lappeenranta, Finland

M. Besancon, F. Couderc, M. Dejardin, D. Denegri, B. Fabbro, J.L. Faure, F. Ferri, S. Ganjour, A. Givernaud, P. Gras, G. Hamel de Monchenault, P. Jarry, E. Locci, J. Malcles, L. Millischer, A. Nayak, J. Rander, A. Rosowsky, M. Titov

DSM/IRFU, CEA/Saclay, Gif-sur-Yvette, France

S. Baffioni, F. Beaudette, L. Benhabib, M. Bluj [16], P. Busson, C. Charlot, N. Daci, T. Dahms, M. Dalchenko, L. Dobrzynski, A. Florent, R. Granier de Cassagnac, M. Haguenauer, P. Miné, C. Mironov, I.N. Naranjo, M. Nguyen, C. Ochando, P. Paganini, D. Sabes, R. Salerno, Y. Sirois, C. Veelken, A. Zabi

Laboratoire Leprince-Ringuet, Ecole Polytechnique, IN2P3-CNRS, Palaiseau, France

J.-L. Agram [17], J. Andrea, D. Bloch, D. Bodin, J.-M. Brom, E.C. Chabert, C. Collard, E. Conte [17], F. Drouhin [17], J.-C. Fontaine [17], D. Gelé, U. Goerlach, C. Goetzmann, P. Juillot, A.-C. Le Bihan, P. Van Hove

Institut Pluridisciplinaire Hubert Curien, Université de Strasbourg, Université de Haute Alsace Mulhouse, CNRS/IN2P3, Strasbourg, France

S. Gadrat

Centre de Calcul de l'Institut National de Physique Nucleaire et de Physique des Particules, CNRS/IN2P3, Villeurbanne, France

S. Beauceron, N. Beaupere, G. Boudoul, S. Brochet, J. Chasserat, R. Chierici, D. Contardo, P. Depasse, H. El Mamouni, J. Fay, S. Gascon, M. Gouzevitch, B. Ille, T. Kurca, M. Lethuillier,

L. Mirabito, S. Perries, L. Sgandurra, V. Sordini, Y. Tschudi, M. Vander Donckt, P. Verdier, S. Viret

Université de Lyon, Université Claude Bernard Lyon 1, CNRS-IN2P3, Institut de Physique Nucléaire de Lyon, Villeurbanne, France

Z. Tsamalaidze [18]

Institute of High Energy Physics and Informatization, Tbilisi State University, Tbilisi, Georgia

C. Autermann, S. Beranek, B. Calpas, M. Edelhoff, L. Feld, N. Heracleous, O. Hindrichs, K. Klein, A. Ostapchuk, A. Perieanu, F. Raupach, J. Sammet, S. Schael, D. Sprenger, H. Weber, B. Wittmer, V. Zhukov [5]

RWTH Aachen University, I. Physikalisches Institut, Aachen, Germany

M. Ata, J. Caudron, E. Dietz-Laursonn, D. Duchardt, M. Erdmann, R. Fischer, A. Güth, T. Hebbeker, C. Heidemann, K. Hoepfner, D. Klingebiel, P. Kreuzer, M. Merschmeyer, A. Meyer, M. Olschewski, K. Padeken, P. Papacz, H. Pieta, H. Reithler, S.A. Schmitz, L. Sonnenschein, J. Steggemann, D. Teyssier, S. Thüer, M. Weber

RWTH Aachen University, III. Physikalisches Institut A, Aachen, Germany

V. Cherepanov, Y. Erdogan, G. Flügge, H. Geenen, M. Geisler, W. Haj Ahmad, F. Hoehle, B. Kargoll, T. Kress, Y. Kuessel, J. Lingemann [2], A. Nowack, I.M. Nugent, L. Perchalla, O. Pooth, A. Stahl

RWTH Aachen University, III. Physikalisches Institut B, Aachen, Germany

M. Aldaya Martin, I. Asin, N. Bartosik, J. Behr, W. Behrenhoff, U. Behrens, M. Bergholz [19], A. Bethani, K. Borras, A. Burgmeier, A. Cakir, L. Calligaris, A. Campbell, S. Choudhury, F. Costanza, C. Diez Pardos, S. Dooling, T. Dorland, G. Eckerlin, D. Eckstein, G. Flucke, A. Geiser, I. Glushkov, P. Gunnellini, S. Habib, J. Hauk, G. Hellwig, D. Horton, H. Jung, M. Kasemann, P. Katsas, C. Kleinwort, H. Kluge, M. Krämer, D. Krücker, E. Kuznetsova, W. Lange, J. Leonard, K. Lipka, W. Lohmann [19], B. Lutz, R. Mankel, I. Marfin, I.-A. Melzer-Pellmann, A.B. Meyer, J. Mnich, A. Mussgiller, S. Naumann-Emme, O. Novgorodova, F. Nowak, J. Olzem, H. Perrey, A. Petrukhin, D. Pitzl, R. Placakyte, A. Raspereza, P.M. Ribeiro Cipriano, C. Riedl, E. Ron, M.Ö. Sahin, J. Salfeld-Nebgen, R. Schmidt [19], T. Schoerner-Sadenius, N. Sen, M. Stein, R. Walsh, C. Wissing

Deutsches Elektronen-Synchrotron, Hamburg, Germany

V. Blobel, H. Enderle, J. Erfle, E. Garutti, U. Gebbert, M. Görner, M. Gosselink, J. Haller, K. Heine, R.S. Höing, G. Kaussen, H. Kirschenmann, R. Klanner, R. Kogler, J. Lange, I. Marchesini, T. Peiffer, N. Pietsch, D. Rathjens, C. Sander, H. Schettler, P. Schleper, E. Schlieckau, A. Schmidt, M. Schröder, T. Schum, M. Seidel, J. Sibille [20], V. Sola, H. Stadie, G. Steinbrück, J. Thomsen, D. Troendle, E. Usai, L. Vanelderen

University of Hamburg, Hamburg, Germany

C. Barth, C. Baus, J. Berger, C. Böser, E. Butz, T. Chwalek, W. De Boer, A. Descroix, A. Dierlamm, M. Feindt, M. Guthoff [2], F. Hartmann [2], T. Hauth [2], H. Held, K.H. Hoffmann, U. Husemann, I. Katkov [5], J.R. Komaragiri, A. Kornmayer [2], P. Lobelle Pardo, D. Martschei, Th. Müller, M. Niegel, A. Nürnberg, O. Oberst, J. Ott, G. Quast, K. Rabbertz, F. Ratnikov, S. Röcker, F.-P. Schilling, G. Schott, H.J. Simonis, F.M. Stober, R. Ulrich, J. Wagner-Kuhr, S. Wayand, T. Weiler, M. Zeise

Institut für Experimentelle Kernphysik, Karlsruhe, Germany

G. Anagnostou, G. Daskalakis, T. Geralis, S. Kesisoglou, A. Kyriakis, D. Loukas, A. Markou, C. Markou, E. Ntomari

Institute of Nuclear and Particle Physics (INPP), NCSR Demokritos, Aghia Paraskevi, Greece

L. Gouskos, T.J. Mertzimekis, A. Panagiotou, N. Saoulidou, E. Stiliaris

University of Athens, Athens, Greece

X. Aslanoglou, I. Evangelou, G. Flouris, C. Foudas, P. Kokkas, N. Manthos, I. Papadopoulos, E. Paradas

University of Ioánnina, Ioánnina, Greece

G. Bencze, C. Hajdu, P. Hidas, D. Horvath [21], B. Radics, F. Sikler, V. Veszpremi, G. Vesztergombi [22], A.J. Zsigmond

KFKI Research Institute for Particle and Nuclear Physics, Budapest, Hungary

N. Beni, S. Czellar, J. Molnar, J. Palinkas, Z. Szillasi

Institute of Nuclear Research ATOMKI, Debrecen, Hungary

J. Karancsi, P. Raics, Z.L. Trocsanyi, B. Ujvari

University of Debrecen, Debrecen, Hungary

S.B. Beri, V. Bhatnagar, N. Dhingra, R. Gupta, M. Kaur, M.Z. Mehta, M. Mittal, N. Nishu, L.K. Saini, A. Sharma, J.B. Singh

Panjab University, Chandigarh, India

Ashok Kumar, Arun Kumar, S. Ahuja, A. Bhardwaj, B.C. Choudhary, S. Malhotra, M. Naimuddin, K. Ranjan, P. Saxena, V. Sharma, R.K. Shivpuri

University of Delhi, Delhi, India

S. Banerjee, S. Bhattacharya, K. Chatterjee, S. Dutta, B. Gomber, Sa. Jain, Sh. Jain, R. Khurana, A. Modak, S. Mukherjee, D. Roy, S. Sarkar, M. Sharan

Saha Institute of Nuclear Physics, Kolkata, India

A. Abdulsalam, D. Dutta, S. Kailas, V. Kumar, A.K. Mohanty [2], L.M. Pant, P. Shukla, A. Topkar

Bhabha Atomic Research Centre, Mumbai, India

T. Aziz, R.M. Chatterjee, S. Ganguly, S. Ghosh, M. Guchait [23], A. Gurtu [24], G. Kole, S. Kumar, M. Maity [25], G. Majumder, K. Mazumdar, G.B. Mohanty, B. Parida, K. Sudhakar, N. Wickramage [26]

Tata Institute of Fundamental Research – EHEP, Mumbai, India

S. Banerjee, S. Dugad

Tata Institute of Fundamental Research – HECR, Mumbai, India

H. Arfaei, H. Bakhshiansohi, S.M. Etesami [27], A. Fahim [28], H. Hesari, A. Jafari, M. Khakzad, M. Mohammadi Najafabadi, S. Paktinat Mehdiabadi, B. Safarzadeh [29], M. Zeinali

Institute for Research in Fundamental Sciences (IPM), Tehran, Iran

M. Grunewald

University College Dublin, Dublin, Ireland

M. Abbrescia [a,b], L. Barbone [a,b], C. Calabria [a,b], S.S. Chhibra [a,b], A. Colaleo [a], D. Creanza [a,c], N. De Filippis [a,c], M. De Palma [a,b], L. Fiore [a], G. Iaselli [a,c], G. Maggi [a,c], M. Maggi [a], B. Marangelli [a,b], S. My [a,c], S. Nuzzo [a,b], N. Pacifico [a], A. Pompili [a,b], G. Pugliese [a,c], G. Selvaggi [a,b], L. Silvestris [a], G. Singh [a,b], R. Venditti [a,b], P. Verwilligen [a], G. Zito [a]

[a] *INFN Sezione di Bari, Bari, Italy*
[b] *Università di Bari, Bari, Italy*
[c] *Politecnico di Bari, Bari, Italy*

G. Abbiendi [a], A.C. Benvenuti [a], D. Bonacorsi [a,b], S. Braibant-Giacomelli [a,b], L. Brigliadori [a,b], R. Campanini [a,b], P. Capiluppi [a,b], A. Castro [a,b], F.R. Cavallo [a], M. Cuffiani [a,b], G.M. Dallavalle [a], F. Fabbri [a], A. Fanfani [a,b], D. Fasanella [a,b], P. Giacomelli [a], C. Grandi [a], L. Guiducci [a,b], S. Marcellini [a], G. Masetti [a,2], M. Meneghelli [a,b], A. Montanari [a], F.L. Navarria [a,b], F. Odorici [a], A. Perrotta [a], F. Primavera [a,b], A.M. Rossi [a,b], T. Rovelli [a,b], G.P. Siroli [a,b], N. Tosi [a,b], R. Travaglini [a,b]

[a] *INFN Sezione di Bologna, Bologna, Italy*
[b] *Università di Bologna, Bologna, Italy*

S. Albergo [a,b], M. Chiorboli [a,b], S. Costa [a,b], F. Giordano [a,2], R. Potenza [a,b], A. Tricomi [a,b], C. Tuve [a,b]

[a] *INFN Sezione di Catania, Catania, Italy*
[b] *Università di Catania, Catania, Italy*

G. Barbagli [a], V. Ciulli [a,b], C. Civinini [a], R. D'Alessandro [a,b], E. Focardi [a,b], S. Frosali [a,b], E. Gallo [a], S. Gonzi [a,b], V. Gori [a,b], P. Lenzi [a,b], M. Meschini [a], S. Paoletti [a], G. Sguazzoni [a], A. Tropiano [a,b]

[a] *INFN Sezione di Firenze, Firenze, Italy*
[b] *Università di Firenze, Firenze, Italy*

L. Benussi, S. Bianco, F. Fabbri, D. Piccolo

INFN Laboratori Nazionali di Frascati, Frascati, Italy

P. Fabbricatore [a], R. Musenich [a], S. Tosi [a,b]

[a] *INFN Sezione di Genova, Genova, Italy*
[b] *Università di Genova, Genova, Italy*

A. Benaglia [a], F. De Guio [a,b], M.E. Dinardo [a,b], S. Fiorendi [a,b], S. Gennai [a], A. Ghezzi [a,b], P. Govoni [a,b], M.T. Lucchini [a,b,2], S. Malvezzi [a], R.A. Manzoni [a,b,2], A. Martelli [a,b,2], D. Menasce [a], L. Moroni [a], M. Paganoni [a,b], D. Pedrini [a], S. Ragazzi [a,b], N. Redaelli [a], T. Tabarelli de Fatis [a,b]

[a] *INFN Sezione di Milano-Bicocca, Milano, Italy*
[b] *Università di Milano-Bicocca, Milano, Italy*

S. Buontempo [a], N. Cavallo [a,c], A. De Cosa [a,b], F. Fabozzi [a,c], A.O.M. Iorio [a,b], L. Lista [a], S. Meola [a,d,2], M. Merola [a], P. Paolucci [a,2]

[a] *INFN Sezione di Napoli, Napoli, Italy*
[b] *Università di Napoli 'Federico II', Napoli, Italy*
[c] *Università della Basilicata (Potenza), Napoli, Italy*
[d] *Università G. Marconi (Roma), Napoli, Italy*

P. Azzi [a], N. Bacchetta [a], D. Bisello [a,b], A. Branca [a,b], R. Carlin [a,b], P. Checchia [a], T. Dorigo [a], U. Dosselli [a], M. Galanti [a,b,2], F. Gasparini [a,b], U. Gasparini [a,b], P. Giubilato [a,b], F. Gonella [a], A. Gozzelino [a], K. Kanishchev [a,c], S. Lacaprara [a], I. Lazzizzera [a,c], M. Margoni [a,b], A.T. Meneguzzo [a,b], F. Montecassiano [a], J. Pazzini [a,b], N. Pozzobon [a,b], P. Ronchese [a,b],

M. Sgaravatto [a], F. Simonetto [a,b], E. Torassa [a], M. Tosi [a,b], P. Zotto [a,b], A. Zucchetta [a,b], G. Zumerle [a,b]

[a] INFN Sezione di Padova, Padova, Italy
[b] Università di Padova, Padova, Italy
[c] Università di Trento (Trento), Padova, Italy

M. Gabusi [a,b], S.P. Ratti [a,b], C. Riccardi [a,b], P. Vitulo [a,b]

[a] INFN Sezione di Pavia, Pavia, Italy
[b] Università di Pavia, Pavia, Italy

M. Biasini [a,b], G.M. Bilei [a], L. Fanò [a,b], P. Lariccia [a,b], G. Mantovani [a,b], M. Menichelli [a], A. Nappi [a,b,†], F. Romeo [a,b], A. Saha [a], A. Santocchia [a,b], A. Spiezia [a,b]

[a] INFN Sezione di Perugia, Perugia, Italy
[b] Università di Perugia, Perugia, Italy

K. Androsov [a,30], P. Azzurri [a], G. Bagliesi [a], J. Bernardini [a], T. Boccali [a], G. Broccolo [a,c], R. Castaldi [a], R.T. D'Agnolo [a,c,2], R. Dell'Orso [a], F. Fiori [a,c], L. Foà [a,c], A. Giassi [a], M.T. Grippo [a,30], A. Kraan [a], F. Ligabue [a,c], T. Lomtadze [a], L. Martini [a,30], A. Messineo [a,b], F. Palla [a], A. Rizzi [a,b], A. Savoy-navarro [a,31], A.T. Serban [a], P. Spagnolo [a], P. Squillacioti [a], R. Tenchini [a], G. Tonelli [a,b], A. Venturi [a], P.G. Verdini [a], C. Vernieri [a,c]

[a] INFN Sezione di Pisa, Pisa, Italy
[b] Università di Pisa, Pisa, Italy
[c] Scuola Normale Superiore di Pisa, Pisa, Italy

L. Barone [a,b], F. Cavallari [a], D. Del Re [a,b], M. Diemoz [a], M. Grassi [a,b,2], E. Longo [a,b], F. Margaroli [a,b], P. Meridiani [a], F. Micheli [a,b], S. Nourbakhsh [a,b], G. Organtini [a,b], R. Paramatti [a], S. Rahatlou [a,b], C. Rovelli [a], L. Soffi [a,b]

[a] INFN Sezione di Roma, Roma, Italy
[b] Università di Roma, Roma, Italy

N. Amapane [a,b], R. Arcidiacono [a,c], S. Argiro [a,b], M. Arneodo [a,c], C. Biino [a], N. Cartiglia [a], S. Casasso [a,b], M. Costa [a,b], P. De Remigis [a], N. Demaria [a], C. Mariotti [a], S. Maselli [a], E. Migliore [a,b], V. Monaco [a,b], M. Musich [a], M.M. Obertino [a,c], N. Pastrone [a], M. Pelliccioni [a,2], A. Potenza [a,b], A. Romero [a,b], M. Ruspa [a,c], R. Sacchi [a,b], A. Solano [a,b], A. Staiano [a], U. Tamponi [a]

[a] INFN Sezione di Torino, Torino, Italy
[b] Università di Torino, Torino, Italy
[c] Università del Piemonte Orientale (Novara), Torino, Italy

S. Belforte [a], V. Candelise [a,b], M. Casarsa [a], F. Cossutti [a,2], G. Della Ricca [a,b], B. Gobbo [a], C. La Licata [a,b], M. Marone [a,b], D. Montanino [a,b], A. Penzo [a], A. Schizzi [a,b], A. Zanetti [a]

[a] INFN Sezione di Trieste, Trieste, Italy
[b] Università di Trieste, Trieste, Italy

S. Chang, T.Y. Kim, S.K. Nam

Kangwon National University, Chunchon, Republic of Korea

D.H. Kim, G.N. Kim, J.E. Kim, D.J. Kong, Y.D. Oh, H. Park, D.C. Son

Kyungpook National University, Daegu, Republic of Korea

J.Y. Kim, Zero J. Kim, S. Song

Chonnam National University, Institute for Universe and Elementary Particles, Kwangju, Republic of Korea

S. Choi, D. Gyun, B. Hong, M. Jo, H. Kim, T.J. Kim, K.S. Lee, S.K. Park, Y. Roh

Korea University, Seoul, Republic of Korea

M. Choi, J.H. Kim, C. Park, I.C. Park, S. Park, G. Ryu

University of Seoul, Seoul, Republic of Korea

Y. Choi, Y.K. Choi, J. Goh, M.S. Kim, E. Kwon, B. Lee, J. Lee, S. Lee, H. Seo, I. Yu

Sungkyunkwan University, Suwon, Republic of Korea

I. Grigelionis, A. Juodagalvis

Vilnius University, Vilnius, Lithuania

H. Castilla-Valdez, E. De La Cruz-Burelo, I. Heredia-de La Cruz [33], R. Lopez-Fernandez, J. Martínez-Ortega, A. Sanchez-Hernandez, L.M. Villasenor-Cendejas

Centro de Investigacion y de Estudios Avanzados del IPN, Mexico City, Mexico

S. Carrillo Moreno, F. Vazquez Valencia

Universidad Iberoamericana, Mexico City, Mexico

H.A. Salazar Ibarguen

Benemerita Universidad Autonoma de Puebla, Puebla, Mexico

E. Casimiro Linares, A. Morelos Pineda, M.A. Reyes-Santos

Universidad Autónoma de San Luis Potosí, San Luis Potosí, Mexico

D. Krofcheck

University of Auckland, Auckland, New Zealand

A.J. Bell, P.H. Butler, R. Doesburg, S. Reucroft, H. Silverwood

University of Canterbury, Christchurch, New Zealand

M. Ahmad, M.I. Asghar, J. Butt, H.R. Hoorani, S. Khalid, W.A. Khan, T. Khurshid, S. Qazi, M.A. Shah, M. Shoaib

National Centre for Physics, Quaid-I-Azam University, Islamabad, Pakistan

H. Bialkowska, B. Boimska, T. Frueboes, M. Górski, M. Kazana, K. Nawrocki, K. Romanowska-Rybinska, M. Szleper, G. Wrochna, P. Zalewski

National Centre for Nuclear Research, Swierk, Poland

G. Brona, K. Bunkowski, M. Cwiok, W. Dominik, K. Doroba, A. Kalinowski, M. Konecki, J. Krolikowski, M. Misiura, W. Wolszczak

Institute of Experimental Physics, Faculty of Physics, University of Warsaw, Warsaw, Poland

N. Almeida, P. Bargassa, C. Beirão Da Cruz E Silva, P. Faccioli, P.G. Ferreira Parracho, M. Gallinaro, J. Rodrigues Antunes, J. Seixas [2], J. Varela, P. Vischia

Laboratório de Instrumentação e Física Experimental de Partículas, Lisboa, Portugal

S. Afanasiev, P. Bunin, I. Golutvin, I. Gorbunov, A. Kamenev, V. Karjavin, V. Konoplyanikov, G. Kozlov, A. Lanev, A. Malakhov, V. Matveev, P. Moisenz, V. Palichik, V. Perelygin, S. Shmatov, N. Skatchkov, V. Smirnov, A. Zarubin

Joint Institute for Nuclear Research, Dubna, Russia

S. Evstyukhin, V. Golovtsov, Y. Ivanov, V. Kim, P. Levchenko, V. Murzin, V. Oreshkin, I. Smirnov, V. Sulimov, L. Uvarov, S. Vavilov, A. Vorobyev, An. Vorobyev

Petersburg Nuclear Physics Institute, Gatchina (St. Petersburg), Russia

Yu. Andreev, A. Dermenev, S. Gninenko, N. Golubev, M. Kirsanov, N. Krasnikov, A. Pashenkov, D. Tlisov, A. Toropin

Institute for Nuclear Research, Moscow, Russia

V. Epshteyn, M. Erofeeva, V. Gavrilov, N. Lychkovskaya, V. Popov, G. Safronov, S. Semenov, A. Spiridonov, V. Stolin, E. Vlasov, A. Zhokin

Institute for Theoretical and Experimental Physics, Moscow, Russia

V. Andreev, M. Azarkin, I. Dremin, M. Kirakosyan, A. Leonidov, G. Mesyats, S.V. Rusakov, A. Vinogradov

P.N. Lebedev Physical Institute, Moscow, Russia

A. Belyaev, E. Boos, A. Demiyanov, A. Ershov, A. Gribushin, O. Kodolova, V. Korotkikh, I. Lokhtin, A. Markina, S. Obraztsov, S. Petrushanko, V. Savrin, A. Snigirev, I. Vardanyan

Skobeltsyn Institute of Nuclear Physics, Lomonosov Moscow State University, Moscow, Russia

I. Azhgirey, I. Bayshev, S. Bitioukov, V. Kachanov, A. Kalinin, D. Konstantinov, V. Krychkine, V. Petrov, R. Ryutin, A. Sobol, L. Tourtchanovitch, S. Troshin, N. Tyurin, A. Uzunian, A. Volkov

State Research Center of Russian Federation, Institute for High Energy Physics, Protvino, Russia

P. Adzic [34], M. Ekmedzic, D. Krpic [34], J. Milosevic

University of Belgrade, Faculty of Physics and Vinca Institute of Nuclear Sciences, Belgrade, Serbia

M. Aguilar-Benitez, J. Alcaraz Maestre, C. Battilana, E. Calvo, M. Cerrada, M. Chamizo Llatas [2], N. Colino, B. De La Cruz, A. Delgado Peris, D. Domínguez Vázquez, C. Fernandez Bedoya, J.P. Fernández Ramos, A. Ferrando, J. Flix, M.C. Fouz, P. Garcia-Abia, O. Gonzalez Lopez, S. Goy Lopez, J.M. Hernandez, M.I. Josa, G. Merino, E. Navarro De Martino, J. Puerta Pelayo, A. Quintario Olmeda, I. Redondo, L. Romero, J. Santaolalla, M.S. Soares, C. Willmott

Centro de Investigaciones Energéticas Medioambientales y Tecnológicas (CIEMAT), Madrid, Spain

C. Albajar, J.F. de Trocóniz

Universidad Autónoma de Madrid, Madrid, Spain

H. Brun, J. Cuevas, J. Fernandez Menendez, S. Folgueras, I. Gonzalez Caballero, L. Lloret Iglesias, J. Piedra Gomez

Universidad de Oviedo, Oviedo, Spain

J.A. Brochero Cifuentes, I.J. Cabrillo, A. Calderon, S.H. Chuang, J. Duarte Campderros, M. Fernandez, G. Gomez, J. Gonzalez Sanchez, A. Graziano, C. Jorda, A. Lopez Virto, J. Marco, R. Marco, C. Martinez Rivero, F. Matorras, F.J. Munoz Sanchez, T. Rodrigo, A.Y. Rodríguez-Marrero, A. Ruiz-Jimeno, L. Scodellaro, I. Vila, R. Vilar Cortabitarte

Instituto de Física de Cantabria (IFCA), CSIC-Universidad de Cantabria, Santander, Spain

D. Abbaneo, E. Auffray, G. Auzinger, M. Bachtis, P. Baillon, A.H. Ball, D. Barney, J. Bendavid, J.F. Benitez, C. Bernet [8], G. Bianchi, P. Bloch, A. Bocci, A. Bonato, O. Bondu, C. Botta,

H. Breuker, T. Camporesi, G. Cerminara, T. Christiansen, J.A. Coarasa Perez, S. Colafranceschi[35], D. d'Enterria, A. Dabrowski, A. David, A. De Roeck, S. De Visscher, S. Di Guida, M. Dobson, N. Dupont-Sagorin, A. Elliott-Peisert, J. Eugster, W. Funk, G. Georgiou, M. Giffels, D. Gigi, K. Gill, D. Giordano, M. Girone, M. Giunta, F. Glege, R. Gomez-Reino Garrido, S. Gowdy, R. Guida, J. Hammer, M. Hansen, P. Harris, C. Hartl, A. Hinzmann, V. Innocente, P. Janot, E. Karavakis, K. Kousouris, K. Krajczar, P. Lecoq, Y.-J. Lee, C. Lourenço, N. Magini, M. Malberti, L. Malgeri, M. Mannelli, L. Masetti, F. Meijers, S. Mersi, E. Meschi, R. Moser, M. Mulders, P. Musella, E. Nesvold, L. Orsini, E. Palencia Cortezon, E. Perez, L. Perrozzi, A. Petrilli, A. Pfeiffer, M. Pierini, M. Pimiä, D. Piparo, M. Plagge, L. Quertenmont, A. Racz, W. Reece, G. Rolandi[36], M. Rovere, H. Sakulin, F. Santanastasio, C. Schäfer, C. Schwick, I. Segoni, S. Sekmen, A. Sharma, P. Siegrist, P. Silva, M. Simon, P. Sphicas[37], D. Spiga, M. Stoye, A. Tsirou, G.I. Veres[22], J.R. Vlimant, H.K. Wöhri, S.D. Worm[38], W.D. Zeuner

CERN, European Organization for Nuclear Research, Geneva, Switzerland

W. Bertl, K. Deiters, W. Erdmann, K. Gabathuler, R. Horisberger, Q. Ingram, H.C. Kaestli, S. König, D. Kotlinski, U. Langenegger, D. Renker, T. Rohe

Paul Scherrer Institut, Villigen, Switzerland

F. Bachmair, L. Bäni, L. Bianchini, P. Bortignon, M.A. Buchmann, B. Casal, N. Chanon, A. Deisher, G. Dissertori, M. Dittmar, M. Donegà, M. Dünser, P. Eller, K. Freudenreich, C. Grab, D. Hits, P. Lecomte, W. Lustermann, B. Mangano, A.C. Marini, P. Martinez Ruiz del Arbol, N. Mohr, F. Moortgat, C. Nägeli[39], P. Nef, F. Nessi-Tedaldi, F. Pandolfi, L. Pape, F. Pauss, M. Peruzzi, F.J. Ronga, M. Rossini, L. Sala, A.K. Sanchez, A. Starodumov[40], B. Stieger, M. Takahashi, L. Tauscher[†], A. Thea, K. Theofilatos, D. Treille, C. Urscheler, R. Wallny, H.A. Weber

Institute for Particle Physics, ETH Zurich, Zurich, Switzerland

C. Amsler[41], V. Chiochia, C. Favaro, M. Ivova Rikova, B. Kilminster, B. Millan Mejias, P. Otiougova, P. Robmann, H. Snoek, S. Taroni, S. Tupputi, M. Verzetti

Universität Zürich, Zurich, Switzerland

M. Cardaci, K.H. Chen, C. Ferro, C.M. Kuo, S.W. Li, W. Lin, Y.J. Lu, R. Volpe, S.S. Yu

National Central University, Chung-Li, Taiwan

P. Bartalini, P. Chang, Y.H. Chang, Y.W. Chang, Y. Chao, K.F. Chen, C. Dietz, U. Grundler, W.-S. Hou, Y. Hsiung, K.Y. Kao, Y.J. Lei, R.-S. Lu, D. Majumder, E. Petrakou, X. Shi, J.G. Shiu, Y.M. Tzeng, M. Wang

National Taiwan University (NTU), Taipei, Taiwan

B. Asavapibhop, N. Suwonjandee

Chulalongkorn University, Bangkok, Thailand

A. Adiguzel, M.N. Bakirci[42], S. Cerci[43], C. Dozen, I. Dumanoglu, E. Eskut, S. Girgis, G. Gokbulut, E. Gurpinar, I. Hos, E.E. Kangal, A. Kayis Topaksu, G. Onengut[44], K. Ozdemir, S. Ozturk[42], A. Polatoz, K. Sogut[45], D. Sunar Cerci[43], B. Tali[43], H. Topakli[42], M. Vergili

Cukurova University, Adana, Turkey

I.V. Akin, T. Aliev, B. Bilin, S. Bilmis, M. Deniz, H. Gamsizkan, A.M. Guler, G. Karapinar[46], K. Ocalan, A. Ozpineci, M. Serin, R. Sever, U.E. Surat, M. Yalvac, M. Zeyrek

Middle East Technical University, Physics Department, Ankara, Turkey

E. Gülmez, B. Isildak [47], M. Kaya [48], O. Kaya [48], S. Ozkorucuklu [49], N. Sonmez [50]

Bogazici University, Istanbul, Turkey

H. Bahtiyar [51], E. Barlas, K. Cankocak, Y.O. Günaydin [52], F.I. Vardarlı, M. Yücel

Istanbul Technical University, Istanbul, Turkey

L. Levchuk, P. Sorokin

National Scientific Center, Kharkov Institute of Physics and Technology, Kharkov, Ukraine

J.J. Brooke, E. Clement, D. Cussans, H. Flacher, R. Frazier, J. Goldstein, M. Grimes, G.P. Heath, H.F. Heath, L. Kreczko, S. Metson, D.M. Newbold [38], K. Nirunpong, A. Poll, S. Senkin, V.J. Smith, T. Williams

University of Bristol, Bristol, United Kingdom

L. Basso [53], A. Belyaev [53], C. Brew, R.M. Brown, D.J.A. Cockerill, J.A. Coughlan, K. Harder, S. Harper, J. Jackson, E. Olaiya, D. Petyt, B.C. Radburn-Smith, C.H. Shepherd-Themistocleous, I.R. Tomalin, W.J. Womersley

Rutherford Appleton Laboratory, Didcot, United Kingdom

R. Bainbridge, O. Buchmuller, D. Burton, D. Colling, N. Cripps, M. Cutajar, P. Dauncey, G. Davies, M. Della Negra, W. Ferguson, J. Fulcher, D. Futyan, A. Gilbert, A. Guneratne Bryer, G. Hall, Z. Hatherell, J. Hays, G. Iles, M. Jarvis, G. Karapostoli, M. Kenzie, R. Lane, R. Lucas [38], L. Lyons, A.-M. Magnan, J. Marrouche, B. Mathias, R. Nandi, J. Nash, A. Nikitenko [40], J. Pela, M. Pesaresi, K. Petridis, M. Pioppi [54], D.M. Raymond, S. Rogerson, A. Rose, C. Seez, P. Sharp †, A. Sparrow, A. Tapper, M. Vazquez Acosta, T. Virdee, S. Wakefield, N. Wardle, T. Whyntie

Imperial College, London, United Kingdom

M. Chadwick, J.E. Cole, P.R. Hobson, A. Khan, P. Kyberd, D. Leggat, D. Leslie, W. Martin, I.D. Reid, P. Symonds, L. Teodorescu, M. Turner

Brunel University, Uxbridge, United Kingdom

J. Dittmann, K. Hatakeyama, A. Kasmi, H. Liu, T. Scarborough

Baylor University, Waco, USA

O. Charaf, S.I. Cooper, C. Henderson, P. Rumerio

The University of Alabama, Tuscaloosa, USA

A. Avetisyan, T. Bose, C. Fantasia, A. Heister, P. Lawson, D. Lazic, J. Rohlf, D. Sperka, J. St. John, L. Sulak

Boston University, Boston, USA

J. Alimena, S. Bhattacharya, G. Christopher, D. Cutts, Z. Demiragli, A. Ferapontov, A. Garabedian, U. Heintz, G. Kukartsev, E. Laird, G. Landsberg, M. Luk, M. Narain, M. Segala, T. Sinthuprasith, T. Speer

Brown University, Providence, USA

R. Breedon, G. Breto, M. Calderon De La Barca Sanchez, S. Chauhan, M. Chertok, J. Conway, R. Conway, P.T. Cox, R. Erbacher, M. Gardner, R. Houtz, W. Ko, A. Kopecky, R. Lander,

O. Mall, T. Miceli, R. Nelson, D. Pellett, F. Ricci-Tam, B. Rutherford, M. Searle, J. Smith, M. Squires, M. Tripathi, S. Wilbur, R. Yohay

University of California, Davis, Davis, USA

V. Andreev, D. Cline, R. Cousins, S. Erhan, P. Everaerts, C. Farrell, M. Felcini, J. Hauser, M. Ignatenko, C. Jarvis, G. Rakness, P. Schlein †, E. Takasugi, P. Traczyk, V. Valuev, M. Weber

University of California, Los Angeles, USA

J. Babb, R. Clare, J. Ellison, J.W. Gary, G. Hanson, H. Liu, O.R. Long, A. Luthra, H. Nguyen, S. Paramesvaran, J. Sturdy, S. Sumowidagdo, R. Wilken, S. Wimpenny

University of California, Riverside, Riverside, USA

W. Andrews, J.G. Branson, G.B. Cerati, S. Cittolin, D. Evans, A. Holzner, R. Kelley, M. Lebourgeois, J. Letts, I. Macneill, S. Padhi, C. Palmer, G. Petrucciani, M. Pieri, M. Sani, V. Sharma, S. Simon, E. Sudano, M. Tadel, Y. Tu, A. Vartak, S. Wasserbaech [55], F. Würthwein, A. Yagil, J. Yoo

University of California, San Diego, La Jolla, USA

D. Barge, R. Bellan, C. Campagnari, M. D'Alfonso, T. Danielson, K. Flowers, P. Geffert, C. George, F. Golf, J. Incandela, C. Justus, P. Kalavase, D. Kovalskyi, V. Krutelyov, S. Lowette, R. Magaña Villalba, N. Mccoll, V. Pavlunin, J. Ribnik, J. Richman, R. Rossin, D. Stuart, W. To, C. West

University of California, Santa Barbara, Santa Barbara, USA

A. Apresyan, A. Bornheim, J. Bunn, Y. Chen, E. Di Marco, J. Duarte, D. Kcira, Y. Ma, A. Mott, H.B. Newman, C. Rogan, M. Spiropulu, V. Timciuc, J. Veverka, R. Wilkinson, S. Xie, Y. Yang, R.Y. Zhu

California Institute of Technology, Pasadena, USA

V. Azzolini, A. Calamba, R. Carroll, T. Ferguson, Y. Iiyama, D.W. Jang, Y.F. Liu, M. Paulini, J. Russ, H. Vogel, I. Vorobiev

Carnegie Mellon University, Pittsburgh, USA

J.P. Cumalat, B.R. Drell, W.T. Ford, A. Gaz, E. Luiggi Lopez, U. Nauenberg, J.G. Smith, K. Stenson, K.A. Ulmer, S.R. Wagner

University of Colorado at Boulder, Boulder, USA

J. Alexander, A. Chatterjee, N. Eggert, L.K. Gibbons, W. Hopkins, A. Khukhunaishvili, B. Kreis, N. Mirman, G. Nicolas Kaufman, J.R. Patterson, A. Ryd, E. Salvati, W. Sun, W.D. Teo, J. Thom, J. Thompson, J. Tucker, Y. Weng, L. Winstrom, P. Wittich

Cornell University, Ithaca, USA

D. Winn

Fairfield University, Fairfield, USA

S. Abdullin, M. Albrow, J. Anderson, G. Apollinari, L.A.T. Bauerdick, A. Beretvas, J. Berryhill, P.C. Bhat, K. Burkett, J.N. Butler, V. Chetluru, H.W.K. Cheung, F. Chlebana, S. Cihangir, V.D. Elvira, I. Fisk, J. Freeman, Y. Gao, E. Gottschalk, L. Gray, D. Green, O. Gutsche, D. Hare, R.M. Harris, J. Hirschauer, B. Hooberman, S. Jindariani, M. Johnson, U. Joshi, B. Klima,

S. Kunori, S. Kwan, J. Linacre, D. Lincoln, R. Lipton, J. Lykken, K. Maeshima, J.M. Marraffino, V.I. Martinez Outschoorn, S. Maruyama, D. Mason, P. McBride, K. Mishra, S. Mrenna, Y. Musienko [56], C. Newman-Holmes, V. O'Dell, O. Prokofyev, N. Ratnikova, E. Sexton-Kennedy, S. Sharma, W.J. Spalding, L. Spiegel, L. Taylor, S. Tkaczyk, N.V. Tran, L. Uplegger, E.W. Vaandering, R. Vidal, J. Whitmore, W. Wu, F. Yang, J.C. Yun

Fermi National Accelerator Laboratory, Batavia, USA

D. Acosta, P. Avery, D. Bourilkov, M. Chen, T. Cheng, S. Das, M. De Gruttola, G.P. Di Giovanni, D. Dobur, A. Drozdetskiy, R.D. Field, M. Fisher, Y. Fu, I.K. Furic, J. Hugon, B. Kim, J. Konigsberg, A. Korytov, A. Kropivnitskaya, T. Kypreos, J.F. Low, K. Matchev, P. Milenovic [57], G. Mitselmakher, L. Muniz, R. Remington, A. Rinkevicius, N. Skhirtladze, M. Snowball, J. Yelton, M. Zakaria

University of Florida, Gainesville, USA

V. Gaultney, S. Hewamanage, L.M. Lebolo, S. Linn, P. Markowitz, G. Martinez, J.L. Rodriguez

Florida International University, Miami, USA

T. Adams, A. Askew, J. Bochenek, J. Chen, B. Diamond, S.V. Gleyzer, J. Haas, S. Hagopian, V. Hagopian, K.F. Johnson, H. Prosper, V. Veeraraghavan, M. Weinberg

Florida State University, Tallahassee, USA

M.M. Baarmand, B. Dorney, M. Hohlmann, H. Kalakhety, F. Yumiceva

Florida Institute of Technology, Melbourne, USA

M.R. Adams, L. Apanasevich, V.E. Bazterra, R.R. Betts, I. Bucinskaite, J. Callner, R. Cavanaugh, O. Evdokimov, L. Gauthier, C.E. Gerber, D.J. Hofman, S. Khalatyan, P. Kurt, F. Lacroix, D.H. Moon, C. O'Brien, C. Silkworth, D. Strom, P. Turner, N. Varelas

University of Illinois at Chicago (UIC), Chicago, USA

U. Akgun, E.A. Albayrak [51], B. Bilki [58], W. Clarida, K. Dilsiz, F. Duru, S. Griffiths, J.-P. Merlo, H. Mermerkaya [59], A. Mestvirishvili, A. Moeller, J. Nachtman, C.R. Newsom, H. Ogul, Y. Onel, F. Ozok [51], S. Sen, P. Tan, E. Tiras, J. Wetzel, T. Yetkin [60], K. Yi

The University of Iowa, Iowa City, USA

B.A. Barnett, B. Blumenfeld, S. Bolognesi, D. Fehling, G. Giurgiu, A.V. Gritsan, G. Hu, P. Maksimovic, M. Swartz, A. Whitbeck

Johns Hopkins University, Baltimore, USA

P. Baringer, A. Bean, G. Benelli, R.P. Kenny III, M. Murray, D. Noonan, S. Sanders, R. Stringer, Q. Wang, J.S. Wood

The University of Kansas, Lawrence, USA

A.F. Barfuss, I. Chakaberia, A. Ivanov, S. Khalil, M. Makouski, Y. Maravin, S. Shrestha, I. Svintradze

Kansas State University, Manhattan, USA

J. Gronberg, D. Lange, F. Rebassoo, D. Wright

Lawrence Livermore National Laboratory, Livermore, USA

A. Baden, B. Calvert, S.C. Eno, J.A. Gomez, N.J. Hadley, R.G. Kellogg, T. Kolberg, Y. Lu, M. Marionneau, A.C. Mignerey, K. Pedro, A. Peterman, A. Skuja, J. Temple, M.B. Tonjes, S.C. Tonwar

University of Maryland, College Park, USA

A. Apyan, G. Bauer, W. Busza, I.A. Cali, M. Chan, L. Di Matteo, V. Dutta, G. Gomez Ceballos, M. Goncharov, Y. Kim, M. Klute, Y.S. Lai, A. Levin, P.D. Luckey, T. Ma, S. Nahn, C. Paus, D. Ralph, C. Roland, G. Roland, G.S.F. Stephans, F. Stöckli, K. Sumorok, D. Velicanu, R. Wolf, B. Wyslouch, M. Yang, Y. Yilmaz, A.S. Yoon, M. Zanetti, V. Zhukova

Massachusetts Institute of Technology, Cambridge, USA

B. Dahmes, A. De Benedetti, G. Franzoni, A. Gude, J. Haupt, S.C. Kao, K. Klapoetke, Y. Kubota, J. Mans, N. Pastika, R. Rusack, M. Sasseville, A. Singovsky, N. Tambe, J. Turkewitz

University of Minnesota, Minneapolis, USA

L.M. Cremaldi, R. Kroeger, L. Perera, R. Rahmat, D.A. Sanders, D. Summers

University of Mississippi, Oxford, USA

E. Avdeeva, K. Bloom, S. Bose, D.R. Claes, A. Dominguez, M. Eads, R. Gonzalez Suarez, J. Keller, I. Kravchenko, J. Lazo-Flores, S. Malik, F. Meier, G.R. Snow

University of Nebraska-Lincoln, Lincoln, USA

J. Dolen, A. Godshalk, I. Iashvili, S. Jain, A. Kharchilava, A. Kumar, S. Rappoccio, Z. Wan

State University of New York at Buffalo, Buffalo, USA

G. Alverson *, E. Barberis, D. Baumgartel, M. Chasco, J. Haley, A. Massironi, D. Nash, T. Orimoto, D. Trocino, D. Wood, J. Zhang

Northeastern University, Boston, USA

A. Anastassov, K.A. Hahn, A. Kubik, L. Lusito, N. Mucia, N. Odell, B. Pollack, A. Pozdnyakov, M. Schmitt, S. Stoynev, K. Sung, M. Velasco, S. Won

Northwestern University, Evanston, USA

D. Berry, A. Brinkerhoff, K.M. Chan, M. Hildreth, C. Jessop, D.J. Karmgard, J. Kolb, K. Lannon, W. Luo, S. Lynch, N. Marinelli, D.M. Morse, T. Pearson, M. Planer, R. Ruchti, J. Slaunwhite, N. Valls, M. Wayne, M. Wolf

University of Notre Dame, Notre Dame, USA

L. Antonelli, B. Bylsma, L.S. Durkin, C. Hill, R. Hughes, K. Kotov, T.Y. Ling, D. Puigh, M. Rodenburg, G. Smith, C. Vuosalo, G. Williams, B.L. Winer, H. Wolfe

The Ohio State University, Columbus, USA

E. Berry, P. Elmer, V. Halyo, P. Hebda, J. Hegeman, A. Hunt, P. Jindal, S.A. Koay, D. Lopes Pegna, P. Lujan, D. Marlow, T. Medvedeva, M. Mooney, J. Olsen, P. Piroué, X. Quan, A. Raval, H. Saka, D. Stickland, C. Tully, J.S. Werner, S.C. Zenz, A. Zuranski

Princeton University, Princeton, USA

E. Brownson, A. Lopez, H. Mendez, J.E. Ramirez Vargas

University of Puerto Rico, Mayaguez, USA

E. Alagoz, D. Benedetti, G. Bolla, D. Bortoletto, M. De Mattia, A. Everett, Z. Hu, M. Jones, K. Jung, O. Koybasi, M. Kress, N. Leonardo, V. Maroussov, P. Merkel, D.H. Miller, N. Neumeister, I. Shipsey, D. Silvers, A. Svyatkovskiy, M. Vidal Marono, F. Wang, L. Xu, H.D. Yoo, J. Zablocki, Y. Zheng

Purdue University, West Lafayette, USA

S. Guragain, N. Parashar

Purdue University Calumet, Hammond, USA

A. Adair, B. Akgun, K.M. Ecklund, F.J.M. Geurts, W. Li, B.P. Padley, R. Redjimi, J. Roberts, J. Zabel

Rice University, Houston, USA

B. Betchart, A. Bodek, R. Covarelli, P. de Barbaro, R. Demina, Y. Eshaq, T. Ferbel, A. Garcia-Bellido, P. Goldenzweig, J. Han, A. Harel, D.C. Miner, G. Petrillo, D. Vishnevskiy, M. Zielinski

University of Rochester, Rochester, USA

A. Bhatti, R. Ciesielski, L. Demortier, K. Goulianos, G. Lungu, S. Malik, C. Mesropian

The Rockefeller University, New York, USA

S. Arora, A. Barker, J.P. Chou, C. Contreras-Campana, E. Contreras-Campana, D. Duggan, D. Ferencek, Y. Gershtein, R. Gray, E. Halkiadakis, D. Hidas, A. Lath, S. Panwalkar, M. Park, R. Patel, V. Rekovic, J. Robles, S. Salur, S. Schnetzer, C. Seitz, S. Somalwar, R. Stone, S. Thomas, M. Walker

Rutgers, The State University of New Jersey, Piscataway, USA

G. Cerizza, M. Hollingsworth, K. Rose, S. Spanier, Z.C. Yang, A. York

University of Tennessee, Knoxville, USA

R. Eusebi, W. Flanagan, J. Gilmore, T. Kamon [61], V. Khotilovich, R. Montalvo, I. Osipenkov, Y. Pakhotin, A. Perloff, J. Roe, A. Safonov, T. Sakuma, I. Suarez, A. Tatarinov, D. Toback

Texas A&M University, College Station, USA

N. Akchurin, J. Damgov, C. Dragoiu, P.R. Dudero, C. Jeong, K. Kovitanggoon, S.W. Lee, T. Libeiro, I. Volobouev

Texas Tech University, Lubbock, USA

E. Appelt, A.G. Delannoy, S. Greene, A. Gurrola, W. Johns, C. Maguire, Y. Mao, A. Melo, M. Sharma, P. Sheldon, B. Snook, S. Tuo, J. Velkovska

Vanderbilt University, Nashville, USA

M.W. Arenton, S. Boutle, B. Cox, B. Francis, J. Goodell, R. Hirosky, A. Ledovskoy, C. Lin, C. Neu, J. Wood

University of Virginia, Charlottesville, USA

S. Gollapinni, R. Harr, P.E. Karchin, C. Kottachchi Kankanamge Don, P. Lamichhane, A. Sakharov

Wayne State University, Detroit, USA

D.A. Belknap, L. Borrello, D. Carlsmith, M. Cepeda, S. Dasu, E. Friis, M. Grothe, R. Hall-Wilton, M. Herndon, A. Hervé, K. Kaadze, P. Klabbers, J. Klukas, A. Lanaro, R. Loveless, A. Mohapatra, M.U. Mozer, I. Ojalvo, G.A. Pierro, G. Polese, I. Ross, A. Savin, W.H. Smith, J. Swanson

University of Wisconsin, Madison, USA

* Corresponding author.
E-mail address: George.Alverson@cern.ch (G. Alverson).
† Deceased.
[1] Also at Vienna University of Technology, Vienna, Austria.
[2] Also at CERN, European Organization for Nuclear Research, Geneva, Switzerland.
[3] Also at Institut Pluridisciplinaire Hubert Curien, Université de Strasbourg, Université de Haute Alsace Mulhouse, CNRS/IN2P3, Strasbourg, France.
[4] Also at National Institute of Chemical Physics and Biophysics, Tallinn, Estonia.
[5] Also at Skobeltsyn Institute of Nuclear Physics, Lomonosov Moscow State University, Moscow, Russia.
[6] Also at Universidade Estadual de Campinas, Campinas, Brazil.
[7] Also at California Institute of Technology, Pasadena, USA.
[8] Also at Laboratoire Leprince-Ringuet, Ecole Polytechnique, IN2P3-CNRS, Palaiseau, France.
[9] Also at Suez Canal University, Suez, Egypt.
[10] Also at Zewail City of Science and Technology, Zewail, Egypt.
[11] Also at Cairo University, Cairo, Egypt.
[12] Also at Fayoum University, El-Fayoum, Egypt.
[13] Also at Helwan University, Cairo, Egypt.
[14] Also at British University in Egypt, Cairo, Egypt.
[15] Now at Ain Shams University, Cairo, Egypt.
[16] Also at National Centre for Nuclear Research, Swierk, Poland.
[17] Also at Université de Haute Alsace, Mulhouse, France.
[18] Also at Joint Institute for Nuclear Research, Dubna, Russia.
[19] Also at Brandenburg University of Technology, Cottbus, Germany.
[20] Also at The University of Kansas, Lawrence, USA.
[21] Also at Institute of Nuclear Research ATOMKI, Debrecen, Hungary.
[22] Also at Eötvös Loránd University, Budapest, Hungary.
[23] Also at Tata Institute of Fundamental Research - HECR, Mumbai, India.
[24] Now at King Abdulaziz University, Jeddah, Saudi Arabia.
[25] Also at University of Visva-Bharati, Santiniketan, India.
[26] Also at University of Ruhuna, Matara, Sri Lanka.
[27] Also at Isfahan University of Technology, Isfahan, Iran.
[28] Also at Sharif University of Technology, Tehran, Iran.
[29] Also at Plasma Physics Research Center, Science and Research Branch, Islamic Azad University, Tehran, Iran.
[30] Also at Università degli Studi di Siena, Siena, Italy.
[31] Also at Purdue University, West Lafayette, USA.
[32] Also at INFN Sezione di Roma, Roma, Italy.
[33] Also at Universidad Michoacana de San Nicolas de Hidalgo, Morelia, Mexico.
[34] Also at Faculty of Physics, University of Belgrade, Belgrade, Serbia.
[35] Also at Facoltà Ingegneria, Università di Roma, Roma, Italy.
[36] Also at Scuola Normale e Sezione dell'INFN, Pisa, Italy.
[37] Also at University of Athens, Athens, Greece.
[38] Also at Rutherford Appleton Laboratory, Didcot, United Kingdom.
[39] Also at Paul Scherrer Institut, Villigen, Switzerland.
[40] Also at Institute for Theoretical and Experimental Physics, Moscow, Russia.
[41] Also at Albert Einstein Center for Fundamental Physics, Bern, Switzerland.
[42] Also at Gaziosmanpasa University, Tokat, Turkey.
[43] Also at Adiyaman University, Adiyaman, Turkey.
[44] Also at Cag University, Mersin, Turkey.
[45] Also at Mersin University, Mersin, Turkey.
[46] Also at Izmir Institute of Technology, Izmir, Turkey.
[47] Also at Ozyegin University, Istanbul, Turkey.
[48] Also at Kafkas University, Kars, Turkey.
[49] Also at Suleyman Demirel University, Isparta, Turkey.
[50] Also at Ege University, Izmir, Turkey.
[51] Also at Mimar Sinan University, Istanbul, Istanbul, Turkey.
[52] Also at Kahramanmaras Sütcü Imam University, Kahramanmaras, Turkey.
[53] Also at School of Physics and Astronomy, University of Southampton, Southampton, United Kingdom.
[54] Also at INFN Sezione di Perugia; Università di Perugia, Perugia, Italy.
[55] Also at Utah Valley University, Orem, USA.
[56] Also at Institute for Nuclear Research, Moscow, Russia.
[57] Also at University of Belgrade, Faculty of Physics and Vinca Institute of Nuclear Sciences, Belgrade, Serbia.
[58] Also at Argonne National Laboratory, Argonne, USA.

[59] Also at Erzincan University, Erzincan, Turkey.
[60] Also at Yildiz Technical University, Istanbul, Turkey.
[61] Also at Kyungpook National University, Daegu, Republic of Korea.